Universidad de Concepción
Dirección de Postgrado
Facultad de Agronomía
Programa de Magíster en Ciencias Agronómicas

EL DWV-A DESENCADENA UNA RESPUESTA DE ESTRÉS GLUTAMATÉRGICA GLIAL RELACIONADA CON EL COLAPSO DEL COMPORTAMIENTO OLFATIVO EN *APIS MELLIFERA*.

Tesis para optar al grado de Magíster en Ciencias Agronómicas

FELIPE BECERRA MOLINA ALEJANDRO
CHILLÁN, CHILE
2026

Profesor Guía: Marisol Vargas
Dpto. de Producción Vegetal
Facultad de Agronomía
Universidad de Concepción

Esta tesis ha sido realizada en el Departamento de Producción Vegetal de la Facultad de Agronomía, Universidad de Concepción.

Profesor Guía

Dra. Marisol Vargas Concha
Facultad de Agronomía
Universidad de Concepción.

Comisión Evaluadora

Dr. Nolberto Arismendi
Facultad de Ciencias
Centro de Investigación Austral Biotech
Universidad Santo Tomás.

Dra. María Dolores López Belchí
Facultad de Agronomía
Universidad de Concepción.

Director de Programa

Dra. Macarena Gerding González
Facultad de Agronomía
Universidad de Concepción

AGRADECIMIENTOS

Agradezco al Fondo Nacional de Desarrollo Científico y Tecnológico (FONDECYT) por financiar mi programa de magíster a través del proyecto N° 1241994, y a la Facultad de Agronomía de la Universidad de Concepción por su respaldo académico e institucional.

Un agradecimiento especial a mi familia y, muy particularmente, a mi madre. Gracias por tu apoyo incondicional, por confiar en mí y por ver mi potencial antes que nadie. Tu convicción y compañía me dieron la fuerza necesaria para formarme como el profesional que soy hoy.

Con todo mi cariño y gratitud, para mi familia Becerra Molina.

TABLA DE CONTENIDOS

Página

ÍNDICE DE TABLAS

ÍNDICE DE FIGURAS

(T=0) in the mediation model. Inference was performed using nonparametric bootstrapping with 500 simulations.

Resumen

El virus de las alas deformadas (DWV-A) es la principal amenaza para la salud de la abeja melífera (*Apis mellifera*), sin embargo, su impacto en los circuitos neuronales que regulan comportamientos ecológicamente relevantes, como la olfacción, sigue siendo poco comprendido. Este estudio evaluó si los déficits olfativos inducidos por el virus se originan a partir de una disfunción periférica sensorial o de un colapso en la neurotransmisión central. Abejas obreras adultas fueron inoculadas oralmente con DWV-A y evaluadas a los 15 días post infección (dpi). Integramos electroantenografía (EAG), olfatometría conductual en tubo en Y, y análisis transcriptómicos de genes claves involucrados en el ciclo glutamato-glutamina y en la plasticidad neuronal. Nuestros resultados demuestran que las altas cargas virales atenúan significativamente la capacidad de detección periférica, lo que se evidencia por una reducción en las amplitudes de EAG en respuesta a volátiles florales complejos de cerezo (*Prunus avium* L.) y arándano (*Vaccinium corymbosum* L.). Curiosamente, este deterioro periférico ocurrió sin cambios transcripcionales significativos en los genes de plasticidad antenal o glutamatérgicos. En contraste, la carga viral cerebral emergió como el principal predictor del desempeño conductual en los ensayos de elección. Los análisis multivariados y de mediación causal revelaron una regulación coordinada al alza de los marcadores gliales *Gln*s y *EaaT-2* en respuesta al aumento de los títulos virales. Esta respuesta transcripcional sigue un patrón de "mediación inconsistente": mientras que *EaaT-2* ejerce un efecto indirecto positivo, sugiriendo un intento homeostático compensatorio para eliminar el exceso de glutamato, este resulta insuficiente para contrarrestar el efecto directo negativo del virus. Proponemos que la replicación viral desencadena una reprogramación metabólica tipo “efecto Warburg", provocando que la hiperinhibición glutamatérgica central colapse el procesamiento olfativo. Estos hallazgos proporcionan un marco novedoso para comprender el deterioro cognitivo crónico impulsado por DWV-A y el desequilibrio ontogenético en las abejas melíferas.

Abstract

Deformed Wing Virus (DWV-A) is a major threat to the health of the honey bee (*Apis mellifera*), yet its impact on the neural circuits governing ecologically relevant behaviors, such as olfaction, remains poorly understood. Thus, this study investigated whether viral-induced olfactory deficits originate from sensory peripheral dysfunction or a collapse in central neurotransmission. Adult worker bees were orally inoculated with DWV-A and evaluated 15 days post-infection (dpi). We integrated electroantennography (EAG), Y-tube behavioral olfactometry, and transcriptomic profiling of key genes involved in the glutamate-glutamine cycle and neuronal plasticity. Our results demonstrate that high viral loads significantly attenuate peripheral detection capacity, evidenced by reduced EAG amplitudes in response to complex floral volatiles from cherry (*Prunus avium* L.) and blueberry (*Vaccinium corymbosum* L.). Interestingly, this peripheral impairment occurred without significant transcriptional changes in antennal plasticity or glutamatergic genes. In contrast, brain viral load emerged as the primary predictor of behavioral failure in choice assays. Multivariate and causal mediation analyses revealed a coordinated upregulation of the glial markers *Gln*s and *EaaT-2* in response to increasing viral titers. This transcriptional response follows an "inconsistent mediation" pattern: while *EaaT-2* exerts a positive indirect effect suggesting a compensatory homeostatic attempt to clear excess glutamate it is insufficient to counteract the negative direct effect of the virus. We propose that viral replication triggers a "Warburg-like" metabolic reprogramming, causing central glutamatergic hyper-inhibition collapses olfactory processing. These findings provide a novel framework for understanding DWV-A driven chronic cognitive impairment and ontogenetic imbalance in honey bees.

CAPÍTULO I.

Introducción General

La polinización mediada por insectos es fundamental para el mantenimiento de la biodiversidad global, garantizando el éxito reproductivo y la calidad de más del 75% de los principales cultivos alimentarios del mundo (Basualdo et al., 2022; Reilly et al., 2020). Este fenómeno no solo garantiza la reproducción de las plantas angiospermas en entornos naturales, sino que también sustenta la arquitectura de la seguridad alimentaria, contribuyendo en la disponibilidad de nutrientes esenciales en la dieta global (van der Sluijs y Vaage, 2016).

En el contexto económico, el valor de la polinización por insectos se traduce en miles de millones de dólares anuales. Específicamente en regiones con una fuerte vocación agroexportadora, como América Latina, el éxito de cultivos de alto valor depende intrínsecamente de la salud y eficiencia de las poblaciones de polinizadores (Garibaldi et al., 2013; Klein et al., 2007). Entre estos, la abeja melífera (*Apis mellifera* L.) destaca como el polinizador generalista más importante debido a su capacidad de forrajeo a gran escala y la facilidad con la que sus colmenas pueden ser manejadas y transportadas hacia áreas de cultivo intensivo (Hristov et al., 2020).

El desempeño de *A. mellifera* es determinante para el éxito productivo de cultivos que definen la matriz económica de zonas templadas. En particular, la producción de frutas como el cerezo (*Prunus avium* L.) y el arándano (*Vaccinium corymbosum* L.) está directamente condicionada por la actividad de las abejas durante los periodos de floración (Mateos-Fierro et al., 2025; Reilly et al., 2020).

Estos cultivos presentan requerimientos específicos de polinización cruzada donde la transferencia de polen entre diferentes variedades es fundamental para el cuajado de los frutos (Klein et al., 2007). La eficiencia de forrajeo de una colmena no depende únicamente de la abundancia de individuos, sino de la integridad neurofisiológica de las abejas recolectoras (Menzel, 2012). Una abeja debe poseer la capacidad de navegar a través de entornos agrícolas complejos, identificar fuentes de recursos florales y comunicar dicha ubicación a sus compañeras (Menzel et al., 2005). Por ello, cualquier factor que afecte las capacidades cognitivas o sensoriales de las abejas puede comprometer la eficiencia de forrajeo, la orientación espacial y la capacidad de

retorno a la colmena, reduciendo potencialmente la actividad de polinización en cultivos dependientes de insectos (Fischer et al., 2014; Tang et al., 2021).

La interacción entre la abeja y su entorno está mediada predominantemente por señales químicas (Knauer y Schiestl, 2015). El sistema olfativo de la abeja melífera es una de las estructuras biológicas más sofisticadas de la naturaleza, permitiéndole detectar y discriminar mezclas complejas de compuestos orgánicos volátiles (VOCs) emitidos por las flores (Wright et al., 2002).

Esta resolución olfativa es la que permite a la abeja distinguir entre variedades de plantas, evaluar la calidad del néctar y aprender de forma asociativa qué olores están vinculados a una recompensa nutricional (Cook et al., 2005; Wright y Schiestl, 2009).

A nivel anatómico y fisiológico, el procesamiento de estas señales comienza en el epitelio antenal. Las antenas, cubiertas de sensilias olfativas, albergan neuronas receptoras olfativas (ORNs) que transducen la señal química en impulsos eléctricos (Sandoz, 2011). Esta información se proyecta posteriormente hacia los lóbulos antenales en el cerebro, donde se forman mapas de actividad glomerular específicos para cada olor, y finalmente a los cuerpos pedunculados (*mushroom bodies*), centros de integración superior responsables del aprendizaje y la memoria olfativa (Sandoz, 2011).

A pesar de la sofisticación de este sistema neurosensorial, su integridad se encuentra amenazada por múltiples estresores ambientales. En las últimas décadas, se ha documentado un declive alarmante en las poblaciones de abejas a nivel mundial, un fenómeno a menudo descrito dentro del marco del Colapso de las Colmenas (CCD) (Genersch et al., 2010; Najib y Hassan, 2021).

Este declive es multifactorial, involucrando la pérdida de hábitat, la fragmentación del paisaje, el uso intensivo de agroquímicos y el cambio climático (Najib y Hassan, 2021; Ochungo et al., 2019). De manera muy prominente, la presión de patógenos emergentes, especialmente los virus de ARN, ha amplificado su impacto debido a la dispersión global del ácaro ectoparásito *Varroa destructor* (Martin et al., 2012). Este ácaro no solo debilita el sistema inmune del huésped, sino que altera drásticamente la dinámica de transmisión viral al inyectar las partículas directamente en los cuerpos grasos de la abeja, eludiendo las barreras digestivas naturales (Posada y Florez et al., 2019; Ramsey et al., 2019). Esta ruta de transmisión directa facilita que

infecciones virales que antes eran encubiertas o asintomáticas se conviertan en epidemias letales para la colmena (De Miranda et al., 2015; Yang y Cox, 2005).

El Virus de las Alas Deformadas (DWV; familia *Ifloviridae*) es el patógeno viral más extendido y económicamente impactante en la apicultura global (Martin y Brettell, 2019). Aunque es conocido por causar deformaciones teratogénicas en las alas de abejas que se infectan durante su desarrollo pupal (de Miranda y Genersch, 2010), su impacto más insidioso ocurre en las abejas adultas que presentan infecciones crónicas (De Miranda et al., 2015). Existen diversas variantes del virus; DWV-A, DWV-B, y DWV-C, siendo DWV-A y DWV-B las más predominantes a nivel mundial (Martin y Brettell, 2019). En Chile, el genotipo DWV-A ha sido identificado como la variante predominante en los apiarios comerciales (Riveros et al., 2019).

A diferencia de otras enfermedades que causan mortalidad aguda, el DWV-A suele generar una degradación progresiva de la salud del hospedero, afectando su longevidad, su metabolismo energético y, de manera crítica, su comportamiento neurobiológico (Chen et al., 2021; Koziy et al., 2019; Traniello et al., 2020). Específicamente, se ha demostrado que esta alteración induce una maduración conductual precoz, modificando los perfiles de expresión génica en el cerebro y forzando a las abejas a realizar tareas de forrajeo prematuras y deficientes (Traniello et al., 2020).

Una característica fundamental del DWV-A es su marcado neurotropismo. Estudios histológicos y moleculares han demostrado que el virus tiene la capacidad de replicarse activamente dentro del tejido nervioso de la abeja, localizándose en áreas clave como los lóbulos antenales y los cuerpos pedunculados (Shah et al., 2009). Esta presencia viral en los centros de integración sensorial sugiere que el virus no solo afecta la salud general del insecto, sino que interfiere directamente con los mecanismos moleculares que regulan la percepción y el procesamiento de la información (Paoli y Galizia, 2021; Pizzorno et al., 2021). Se ha observado que la infección sostenida con la variante DWV-A reduce la sensibilidad olfativa y altera la transcripción de genes vinculados con la percepción de señales químicas en las abejas (Diego et al., 2024; Silva et al., 2021). Sin embargo, la relación directa entre la replicación viral a nivel central y la maquinaria molecular que regula la neurotransmisión sigue estando insuficientemente caracterizada. El procesamiento de

la información olfativa dentro de los centros de integración cerebral depende de una estricta regulación de neurotransmisores (Sandoz, 2011). Si bien aminas biogénicas como la octopamina participan en el aprendizaje asociativo (Farooqui et al., 2003; Hammer, 1993), el glutamato actúa como el principal neurotransmisor excitatorio en los circuitos neuronales primarios de los lóbulos antenales y los cuerpos pedunculados, siendo crítico para la transducción inicial y el procesamiento de las señales olfativas (Barbara et al., 2005; Bicker, 1999).

Mantener niveles óptimos de glutamato es indispensable para asegurar una señalización sináptica confiable y prevenir la excitotoxicidad (Meldrum, 2000; Menzel, 2012). Aunque el neurotropismo del DWV-A en el cerebro de la abeja está bien documentado, actualmente no existen datos disponibles sobre cómo la carga viral afecta la transcripción de los componentes responsables de la síntesis, el transporte y la recepción de este neurotransmisor. En consecuencia, determinar el impacto de la infección por DWV-A en la expresión de elementos clave del sistema glutamatérgico es esencial para dilucidar la base molecular de la disfunción neurofisiológica observada en *A. mellifera*.

HIPÓTESIS

Las altas cargas virales de la variante A del Virus de las Alas Deformadas (DWV-A) a nivel central en *A. mellifera* alteran la transcripción de componentes estructurales y funcionales del sistema glutamatérgico, desregulando la homeostasis de este neurotransmisor y contribuyendo a la disfunción neurofisiológica de los centros de integración olfativa.

OBJETIVO GENERAL

Evaluar la relación entre la respuesta conductual olfativa y la sensibilidad olfativa periférica en abejas melíferas (*A. mellifera*) infectadas con el Virus de las Alas Deformadas variante A (DWV-A) frente a compuestos volátiles complejos de origen agrícola y compuestos volátiles puros.

OBJETIVOS ESPECÍFICOS

- Determinar la relación entre las cargas virales de DWV-A y los niveles de transcripción de componentes del sistema glutamatérgico a nivel central, comparando abejas del grupo control (N-DWV-A) y del grupo inoculado (I-DWV-A).
- Evaluar la sensibilidad olfativa periférica mediante electroantenografía (EAG) frente al compuesto volátil puro (1,4-cineol), compuestos volátiles complejos (arándano y cerezo) y la mezcla (cerezo + 1,4-cineol), comparando las amplitudes de respuesta entre abejas de los grupos N-DWV-A e I-DWV-A.
- Evaluar la respuesta conductual olfativa mediante ensayos en olfatómetro de tubo en Y frente a compuestos volátiles complejos (arándano y cerezo), al compuesto volátil puro (1,4-cineol) y a la mezcla (cerezo + 1,4-cineol), comparando el desempeño de abejas de los grupos N-DWV-A e I-DWV-A.

REFERENCIAS CITADAS

Barbara, G.S., Zube, C., Rybak, J., Gauthier, M., Grünewald, B. 2005. Acetylcholine, GABA and glutamate induce ionic currents in cultured antennal lobe neurons of the honeybee, *Apis mellifera*. J Comp Physiol A Neuroethol Sens Neural Behav Physiol. 191(9): 823-836.

Basualdo, M., Cavigliasso, P., de Avila, R.S., Aldea-Sánchez, P., Correa-Benítez, A., Harms, J.M., Ramos, A.K., Rojas-Bravo, V., Salvarrey, S. 2022. Current status and economic value of insect-pollinated dependent crops in Latin America. Ecological Economics. 196.

Bicker, G. 1999. Histochemistry of classical neurotransmitters in antennal lobes and mushroom bodies of the honeybee. Microsc Res Tech. 45(3): 174-183.

Chen, P., Lu, Y.H., Lin, Y.H., Wu, C.P., Tang, C.K., Wei, S.C., Wu, Y.L. 2021. Deformed wing virus infection affects the neurological function of *Apis mellifera* by altering extracellular adenosine signaling. Insect Biochem Mol Biol. 139: 103674.

Cook, S.M., Sandoz, J.C., Martin, A.P., Murray, D.A., Poppy, G.M., Williams, I.H. 2005. Could learning of pollen odours by honey bees (*Apis mellifera*) play a role in their foraging behaviour? Physiological Entomology. 30(2): 164-174.

De Miranda, J.R., Bailey, L., Ball, B.V., Blanchard, P., Budge, G.E., Chejanovsky, N., Chen, Y.P., Gauthier, L., Genersch, E., de Graaf, D.C., Ribière, M., Ryabov, E., De Smet, L., van der Steen, J.J.M. 2015. Standard methods for virus research in *Apis mellifera*. Journal of Apicultural Research. 52(4): 1-56.

De Miranda, J.R., Genersch, E. 2010. Deformed wing virus. Journal of Invertebrate Pathology. 103: S48-S61.

Diego, S., Nolberto, A., Pablo, A.J., Ricardo, C., Nelson, Z., Marisol, V. 2024. Nursing Honeybee Behavior and Sensorial-Related Genes Are Altered by Deformed Wing Virus Variant A. Insects. 15(2).

Farooqui, T., Robinson, K., Vaessin, H., Smith, B.H. 2003. Modulation of early olfactory processing by an octopaminergic reinforcement pathway in the honeybee. J Neurosci. 23(12): 5370-5380.

Fischer, J., Müller, T., Spatz, A.K., Greggers, U., Grünewald, B., Menzel, R. 2014. Neonicotinoids Interfere with Specific Components of Navigation in Honeybees. PLoS One. 9(3): e91364.

Garibaldi, L.A., Steffan-Dewenter, I., Winfree, R., Aizen, M.A., Bommarco, R., Cunningham, S.A., Kremen, C., Carvalheiro, L.G., Harder, L.D., Afik, O., Bartomeus, I., Benjamin, F., Boreux, V., Cariveau, D., Chacoff, N.P., Dudenhöffer, J.H., Freitas, B.M., Ghazoul, J., Greenleaf, S., Klein, A.M. 2013. Wild pollinators enhance fruit set of crops regardless of honey bee abundance. Science. 339(6127): 1608-1611.

Genersch, E., von der Ohe, W., Kaatz, H., Schroeder, A., Otten, C., Büchler, R., Berg, S., Ritter, W., Mühlen, W., Gisder, S., Meixner, M., Liebig, G., Rosenkranz, P. 2010. The German bee monitoring project: a long term study to understand periodically high winter losses of honey bee colonies. Apidologie. 41(3): 332-352.

Hammer, M. 1993. An identified neuron mediates the unconditioned stimulus in associative olfactory learning in honeybees. Nature. 366: 59-63.

Hristov, P., Neov, B., Shumkova, R., Palova, N. 2020. Significance of Apoidea as Main Pollinators. Ecological and Economic Impact and Implications for Human Nutrition. Diversity. 12(7).

Klein, A.M., Vaissière, B.E., Cane, J.H., Steffan-Dewenter, I., Cunningham, S.A., Kremen, C., Tscharntke, T. 2007. Importance of pollinators in changing landscapes for world crops. Proc Biol Sci. 274(1608): 303-313.

Knauer, A.C., Schiestl, F.P. 2015. Bees use honest floral signals as indicators of reward when visiting flowers. Ecology Letters. 18(2): 135-143.

Koziy, R.V., Wood, S.C., Kozii, I.V., van Rensburg, C.J., Moshynskyy, I., Dvylyuk, I., Simko, E. 2019. Deformed Wing Virus Infection in Honey Bees (*Apis mellifera* L.). Vet Pathol. 56(4): 636-641.

Martin, S.J., Brettell, L.E. 2019. Deformed Wing Virus in Honeybees and Other Insects. Annu Rev Virol. 6(1): 49-69.

Martin, S.J., Highfield, A.C., Brettell, L., Villalobos, E.M., Budge, G.E., Powell, M., Nikaido, S., Schroeder, D.C. 2012. Global Honey Bee Viral Landscape Altered by a Parasitic Mite. Science. 336(6086): 1304-1306.

Mateos-Fierro, Z., Garratt, M.P.D., Fountain, M.T., Ashbrook, K., Westbury, D.B. 2025. Contribution of pollinators to delivering fruit quality in commercial sweet cherry orchards. JSFA reports. 5(8): 330-336.

Menzel, R. 2012. The honeybee as a model for understanding the basis of cognition. Nat Rev Neurosci. 13(11): 758-768.

Menzel, R., Greggers, U., Smith, A., Berger, S., Brandt, R., Brunke, S., Bundrock, G., Hülse, S., Plümpe, T., Schaupp, F., Schüttler, E., Stach, S., Stindt, J., Stollhoff, N., Watzl, S. 2005. Honey bees navigate according to a map-like spatial memory. Proceedings of the National Academy of Sciences. 102(8): 3040-3045.

Najib, K.L., Hassan, A.S. 2021. Food and environmental degradation as causative agents of honey bee colonies decline: Mathematical model approach. Journal of the Nigerian Society of Physical Sciences. 446-454.

Ochungo, P., Veldtman, R., Abdel-Rahman, E.M., Raina, S., Muli, E., Landmann, T. 2019. Multi-sensor mapping of honey bee habitats and fragmentation in agro-ecological landscapes in Eastern Kenya. Geocarto International. 36(8): 839-860.

Paoli, M., Galizia, G.C. 2021. Olfactory coding in honeybees. Cell Tissue Res. 383(1): 35-58.

Pizzorno, M.C., Field, K., Kobokovich, A.L., Martin, P.L., Gupta, R.A., Mammone, R., Rovnyak, D., Capaldi, E.A. 2021. Transcriptomic Responses of the Honey Bee Brain to Infection with Deformed Wing Virus. Viruses. 13(2).

Posada-Florez, F., Childers, A.K., Heerman, M.C., Egekwu, N.I., Cook, S.C., Chen, Y., Evans, J.D., Ryabov, E.V. 2019. Deformed wing virus type A, a major honey bee pathogen, is vectored by the mite *Varroa destructor* in a non-propagative manner. Scientific Reports. 9(1): 12445.

Ramsey, S.D., Ochoa, R., Bauchan, G., Gulbronson, C., Mowery, J.D., Cohen, A., Lim, D., Joklik, J., Cicero, J.M., Ellis, J.D., Hawthorne, D., van Engelsdorp, D. 2019. *Varroa destructor* feeds primarily on honey bee fat body tissue and not hemolymph. Proceedings of the National Academy of Sciences. 116(5): 1792-1801.

Reilly, J.R., Artz, D.R., Biddinger, D., Bobiwash, K., Boyle, N.K., Brittain, C., Brokaw, J., Campbell, J.W., Daniels, J., Elle, E., Ellis, J.D., Fleischer, S.J., Gibbs, J., Gillespie, R.L., Gundersen, K.B., Gut, L., Hoffman, G., Joshi, N., Lundin, O., Winfree, R. 2020. Crop production in the USA is frequently limited by a lack of pollinators. Proc Biol Sci. 287(1931): 20200922.

Riveros, G., Arismendi, N., Zapata, N., Evans, D., Pérez, I., Aldea, P., Vargas, M. 2019. Occurrence, prevalence and viral load of deformed wing virus variants in *Apis mellifera* colonies in Chile. Journal of Apicultural Research. 59: 1-6.

Sandoz, J.C. 2011. Behavioral and neurophysiological study of olfactory perception and learning in honeybees. Front Syst Neurosci. 5: 98.

Shah, K.S., Evans, E.C., Pizzorno, M.C. 2009. Localization of deformed wing virus (DWV) in the brains of the honeybee, *Apis mellifera* Linnaeus. Virology Journal. 6(1).

Silva, D., Ceballos, R., Arismendi, N., Dalmon, A., Vargas, M. 2021. Variant A of the Deformed Wings Virus Alters the Olfactory Sensitivity and the Expression of Odorant Binding Proteins on Antennas of *Apis mellifera*. Insects. 12(10).

Tang, C.K., Lin, Y.H., Jiang, J.A., Lu, Y.H., Tsai, C.H., Lin, Y.C., Chen, Y.R., Wu, C.P., Wu, Y.L. 2021. Real-time monitoring of deformed wing virus-infected bee foraging behavior following histone deacetylase inhibitor treatment. iScience. 24(10).

Traniello, I.M., Bukhari, S.A., Kevill, J., Ahmed, A.C., Hamilton, A.R., Naeger, N.L., Schroeder, D.C., Robinson, G.E. 2020. Meta-analysis of honey bee neurogenomic response links Deformed wing virus type A to precocious behavioral maturation. Sci Rep. 10(1): 3101.

Van der Sluijs, J.P., Vaage, N.S. 2016. Pollinators and Global Food Security: the Need for Holistic Global Stewardship. Food Ethics. 1(1): 75-91.

Wright, G.A., Schiestl, F.P. 2009. The evolution of floral scent: the influence of olfactory learning by insect pollinators on the honest signalling of floral rewards. Functional Ecology. 23(5): 841-851.

Wright, G.A., Skinner, B.D., Smith, B.H. 2002. Ability of honeybee, *Apis mellifera*, to detect and discriminate odors of varieties of canola (*Brassica rapa* and *Brassica napus*) and snapdragon flowers (*Antirrhinum majus*). Journal of chemical ecology. 28(4): 721-740.

Yang, X., Cox, D.L. 2005. Impact of an ectoparasite on the immunity and pathology of an invertebrate: Evidence for host immunosuppression and viral amplification. Proceedings of the National Academy of Sciences. 102(21): 7470-7475.

CAPÍTULO II.

Manuscrito enviado a Frontiers in Cellular and Infection Microbiology, sección Molecular Viral Pathogenesis.

Deformed Wing Virus Variant A Triggers a Glutamatergic Stress Response Linked to Olfactory Behavioral Collapse in *Apis mellifera*.

F. Becerra[1], D. Silva[1,2], Y. Fuentes[1], D. Villa[1], N. Arismendi[3], R. Ceballos[4], C. Gomez-Diaz[2], M. Vargas[1*]

[1]Laboratorios de Virología y Neurociencia en Abejas, Facultad de Agronomía, Universidad de Concepción, Chillán, Chile.
[2]Departamento de Biología Funcional (Área de Genética), Facultad de Medicina y Ciencias de la Salud, Universidad de Oviedo, Oviedo, España.
[3]Centro de Investigación Austral Biotech, Facultad de Ciencias, Universidad Santo Tomás, Temuco, Chile.
[4]Laboratorio de Ecología Química, Instituto de Investigaciones Agropecuarias, INIA Quilamapu, Chillán, Chile.

Correspondence
M. Vargas*marisolvargas@udec.cl

Keywords: *Apis mellifera*, Deformed Wing Virus A, glutamatergic stress, antenna, behavior

ABSTRACT

Deformed Wing Virus (DWV-A) is a major threat to the health of the honey bee (*Apis mellifera*), yet its impact on the neural circuits governing ecologically relevant behaviors, such as olfaction, remains poorly understood. Thus, this study investigated the extent to which virus induced olfactory deficits are driven by peripheral sensory dysfunction or a collapse in central neurotransmission. Adult worker bees were orally inoculated with DWV-A and evaluated 15 days post-infection (dpi). We integrated electroantennography (EAG), Y-tube behavioral olfactometry, and transcriptomic profiling of key genes involved in the glutamate-glutamine cycle and neuronal plasticity. Our results demonstrate that high viral loads significantly attenuate peripheral detection capacity, evidenced by reduced EAG amplitudes in response to complex floral volatiles from cherry (*Prunus avium* L.) and blueberry (*Vaccinium corymbosum* L.). Interestingly, this peripheral impairment occurred without significant transcriptional changes in synaptic plasticity or glutamatergic genes within the evaluated whole tissues. In contrast, whole head viral load emerged as the primary predictor of behavioral failure in choice assays. Multivariate and causal mediation analyses revealed a coordinated upregulation of the glutamate clearance and metabolism genes *Gs2* and *Eaat2* in response to increasing viral titers. This transcriptional response follows an "inconsistent mediation" pattern: while *Eaat2* exerts a positive indirect effect suggesting a compensatory homeostatic attempt to clear excess glutamate it is insufficient to counteract the negative direct effect of the virus. We propose that viral replication triggers a "Warburg like" metabolic reprogramming, causing central glutamatergic hyper inhibition and collapsing olfactory processing. These findings provide a novel framework for understanding DWV-A driven chronic cognitive impairment and homeostatic failure in honey bees.

1. INTRODUCTION

Insect mediated pollination is a determining factor for the yield and quality of high economic value crops, such as blueberry (*Vaccinium corymbosum* L.) and cherry (*Prunus avium* L.) (Basualdo et al., 2022; Mateos-Fierro et al., 2025; Reilly et al.,

2020). The foraging efficiency of the honey bee (*Apis mellifera* L.) in these agricultural systems depends on its neurophysiological capacity to detect and discriminate complex mixtures of volatile organic compounds (VOCs) emitted by flowers (Menzel, 2012). This olfactory resolution directly modulates the processing of chemical signals, ranging from the generalization of VOCs among closely related varieties (Wright et al., 2002) to the rapid learning and fine discrimination of odors associated with specific rewards, such as pollen (Cook et al., 2005). The transduction of these chemical signals occurs in the antennae, from where the information projects to the antennal lobes and the mushroom bodies in the brain (Paoli & Galizia, 2021). At the central level, olfactory coding and memory formation are modulated by a complex neurochemical network where cholinergic and aminergic pathways particularly dopamine drive primary synaptic plasticity mechanisms in insects (Menzel, 2012; Schwaerzel et al., 2003). Within this network, the glutamatergic system contributes to synaptic refinement, with NMDA type receptors being implicated in the consolidation and stabilization of olfactory memories (Xia et al., 2005). This adaptive processing depends on coordination between the neurotransmitter cycle, its clearance, and the activation of postsynaptic receptors (Kucharski et al., 2000; Shah et al., 2018).

Deformed Wing Virus (DWV; Iflavirus), transmitted primarily by the ectoparasitic mite *Varroa destructor*, stands as one of the most globally prevalent pathogens strongly associated with the winter collapse of *A. mellifera* colonies (Paxton et al., 2022). Its widespread impact is well documented; DWV has emerged as the most prevalent insect virus globally, with studies estimating that it infects a minimum average of 55% of honey bee colonies worldwide across dozens of countries (Martin & Brettell, 2019). Although both DWV-A and DWV-B variants have been reported in Chile, the DWV-A genotype has been identified as the most predominant variant in apiaries (Riveros et al., 2019). The neurovirulence of this pathogen is characterized by pronounced neurotropism; studies such as Shah et al. (2009) have evidenced active viral replication within key sensory integration centers, including the antennal lobes and mushroom bodies. Sustained infection with the DWV-A variant reduces olfactory sensitivity and alters the transcription of genes linked with chemical signal perception in honey bees (Silva et al., 2024; Silva et al., 2021). However, the relationship

between central viral replication and the molecular machinery regulating neurotransmission remains poorly characterized. Olfactory information processing within brain integration centers relies on the precise balance of diverse neurotransmitter systems to ensure reliable synaptic signaling. Specifically, the tight regulation of extracellular glutamate is critical to preserve signal to noise ratios (Liu & Wilson, 2013) and prevent excitotoxicity. Although the neurotropism of DWV-A in the honey bee brain has been reported, no data are currently available on how viral load affects the transcription of components responsible for glutamate synthesis, clearance, and receptor signaling. Consequently, determining the impact of DWV-A infection on the expression of key elements of the glutamatergic system is essential for elucidating the molecular basis of the neurophysiological dysfunction observed in *A. mellifera*.

2. MATERIALS AND METHODS

Viral Inoculum Preparation

The inoculum of the Deformed Wing Virus variant A (DWV-A) was prepared following the protocols described by Gusachenko et al. (2020) and Silva et al. (2024). The viral inoculum was obtained from field honey bee colonies maintained in an experimental apiary. Colonies were previously screened by quantitative PCR (qPCR) to determine the presence and viral load of Deformed Wing Virus variant A (DWV-A). In parallel, the presence of other pathogens, *Nosema* spp*., Lotmaria* spp., DWV-B, Acute Bee Paralysis Virus (ABPV), and Chronic Bee Paralysis Virus (CBPV), were also assessed. The selection of the colony used for viral inoculum preparation was based on viral quantification criteria, including a Cq value < 15 for DWV-A and Cq values > 32 for the other pathogens described above. A group of 20 symptomatic bees was homogenized in phosphate buffered saline (1X PBS) for 90 seconds at high speed using a Stomacher 80 laboratory blender (Seward, London, UK). The homogenate was then centrifuged twice: first at 1500× g for 10 minutes, followed by 10,000× g for 10 minutes, both at 4°C. The supernatant was purified by filtration through a 0.22 µM filter (PES, Merck Millipore, Darmstadt, Germany). To determine the exact concentration of viral particles present in the inoculum, a 200 µL aliquot of the supernatant was collected for RNA extraction, cDNA synthesis, and subsequent quantification of the

viral load via qPCR, following the methodology detailed in the RNA extraction section. The remaining extracted inoculum was stored at -80°C until further use.

Viral Inoculation

Adult worker honey bees used in all experimental procedures were obtained from the apiary of the experimental station "El Nogal" (36°35′58.25″ S, 72°04′51.77″ W), University of Concepción, Chillán, Chile. Donor colonies were preselected based on pathogen screening, prioritizing those free from *Nosema ceranae* (Ct > 32), *Lotmaria passim* (Ct > 32), and exhibiting either undetectable or minimal viral loads of acute bee paralysis virus (ABPV, Ct > 32), chronic bee paralysis virus (CBPV, Ct > 32), and DWV (Ct > 32). The selected brood frames were then maintained in the laboratory under controlled environmental conditions (30 °C ± 1; 60% ± 3% relative humidity) until adult emergence. Newly emerged worker bees (< 24 h old) were carefully collected from these frames and randomly assigned to plastic cages (base diameter: 8 cm, top diameter: 10 cm, height: 15 cm), following the general experimental setup described by Silva et al. (2021). Briefly, newly emerged bees (24 h) from the brood frames were orally inoculated with the viral suspension (I-DWV Treatment), following the methodologies described by Silva et al. (2024), Hsieh et al. (2020), and de Miranda et al. (2015) with minor modifications as detailed below. Each bee received 5 µL of the viral suspension (1.0×10^{9} copy number per bee) diluted in a 60% sucrose solution. Bees that did not fully consume the viral suspension were excluded from the experiment. Non-inoculated bees served as the control group (N-DWV Treatment), individually receiving only 5 µL of a virus free 60% sucrose solution.

In total, 720 worker bees were used across three independent trials. In each trial, bees were distributed among four replicates for the two treatments, with 30 bees per cage. Each plastic cage was provided with a 3 g supplement of a pollen substitute (comprising soy, brewer's yeast, corn starch, wheat flour, corbicular pollen, and canola oil) and 60% sucrose syrup *ad libitum*, following the recommendations of Arismendi et al. (2020).

Floral Volatile Collection, Chemical Characterization, and Stimuli Preparation

For the preparation of floral stimuli used in the bioassays, fresh cherry (*P. avium* L.) and blueberry (*V. corymbosum* L.) flowers were collected manually at the "El Nogal" Experimental Station (University of Concepción, Chillán, Chile). Collections were performed by selecting representative branches during the flowering period, within a consistent time window (09:00-12:00 h), across two independent sampling events synchronized with the peak bloom. Only plants in full anthesis (> 50% open flowers) were included. Immediately upon cutting, samples were placed in tightly closed transparent plastic bags and kept in a cooler in the field. Upon arrival at the laboratory, they were stored at 4 °C to prevent desiccation and preserve floral volatiles until use.

The volatile fraction of the flower samples was collected using the dynamic headspace method, following the methodology described by Silva et al. (2025). Fifty grams of fresh flowers were encapsulated in a 600 mL Pyrex glass chamber. Volatile compounds were adsorbed using a 200 mg Porapak Q trap (80-100 mesh), previously cleaned with 1 mL of anhydrous ether and thermally conditioned at 220 °C for 2 h under a constant nitrogen flow of 60 mL min^{-1}. Collection was carried out for 24 h at room temperature (22 ± 2 °C) using a positive/negative air pressure system, with an inlet flow of 0.5 L min^{-1} and an outlet flow of 0.45 L min^{-1}. The air entering the system was purified through an activated charcoal filter. Volatiles were extracted from the Porapak Q traps by elution with 1 mL of chromatographic grade hexane.

For relative quantification, 10 mg L^{-1} of Tetralin was used as an internal standard. Compound characterization and relative quantification were performed using gas chromatography mass spectrometry (GC-MS) (GC-MS QP2010 Plus; Shimadzu), equipped with an InertCap 5MS capillary column (5% Diphenyl 95% Dimethylpolysilarylene, 60 m x 0.25 mm i.d. x 0.25 µm film thickness; GL Science, Japan). Helium was used as the carrier gas at a flow rate of 1.4 mL min^{-1}. The oven temperature program started at 40 °C (held for 1 min), followed by a temperature ramp of 10 °C min^{-1} up to 280 °C, which was held for 10 min.

Volatiles were identified by comparing mass spectra with the NIST 2.0 library and by calculating Kovats retention indices (RI). The eluates were stored in amber vials at -40 °C. For the bioassays, the mixture treatment was prepared by combining the cherry

volatile fraction with a commercial standard of 1,4-cineole (CAS: 470-67-7; Sigma-Aldrich, St. Louis, MO, USA). The standard was previously adjusted to a concentration of 1,000 ppm using hexane as a solvent.

Evaluation of Olfactory Reception

Electroantennography (EAG) was used to determine the olfactory reception of 15 day old adult worker *A. mellifera* (evaluated at 15 days post-viral inoculation) assigned to one of two treatments (I-DWV and N-DWV). The olfactory stimulus panel included complex volatile fractions collected from cherry (*P. avium* L.) and blueberry (*V. corymbosum* L.) flowers, a mixture of cherry volatiles + 1,4-cineole, and pure 1,4-cineole, which was included as a control for the EAG assay. Each stimulus was evaluated on five bees per treatment.

The head with its attached antennae served as the receptor organ, adapting the methodology described by Silva et al. (2021). The whole head was removed from the insect's body using a scalpel, and only the first distal segment of the recording antenna was cut with dissection scissors to facilitate electrical contact. This head antenna preparation was then mounted between two glass electrodes filled with a conductive saline solution consisting of KCl (0.1 M) and polyvinylpyrrolidone (0.1%). Following stimulation and data acquisition, the entire head (including both antennae) was immediately stored at -80 °C for subsequent molecular analysis.

A 10 µL volume of each stimulus was applied to filter paper (Whatman No. 1, Whatman®, Sigma-Aldrich, Darmstadt, Germany). The stimulus was delivered to the antenna via a stimulus controller (CS-55, Syntech, Hilversum, Netherlands) with an airflow of 40 mL s^{-1} and a duration of 0.2 s, with an interval of at least 30 s between stimulations to allow for the recovery of basal antennal signals. Each antenna was stimulated three times per stimulus; additionally, each antenna was stimulated with a blank (air) and hexane (≥ 99% GC, Sigma-Aldrich, Munich, Germany).

Data were recorded using EAG 2025 software (Syntech, Hilversum, Netherlands) for the acquisition and analysis of depolarizations obtained during electroantennography. To correlate the DWV-A viral load with the electrophysiological response to volatile stimuli, RNA extraction, subsequent cDNA synthesis, and viral load quantification via

qPCR were performed on the heads of the bees from each treatment following the procedure of Vargas et al. (2017). Additionally, to evaluate molecular changes, the expression of neuronal plasticity genes (*CAMKII*, *PKC*, *CPeb2*, *CalpC*, and *CalpB*) and glutamate homeostasis genes (*Gs2*, *Eaat1*, *Eaat2*, and *Eaat3*) was analyzed (Table 1).

Behavioral Assays

The behavioral response of worker honey bees in the I-DWV and N-DWV treatments were evaluated Y-tube olfactometry. Glass Y-tube olfactometers (21 cm long with a 3 cm internal diameter) (University of Concepción, Concepción, Chile) were custom built with glass odor chambers (15 cm long with a 3 cm internal diameter) connected to the ends of the central arms to deliver the stimulus using a filtered airflow at 280 mL min^{-1} generated by a positive pressure air pump.

A filter paper strip (1 cm x 7.5 cm) was loaded with 10 µL of each stimulus. Floral fractions of cherry (*P. avium* L.) and blueberry (*V. corymbosum* L.) were applied after dilution in hexane, while the mixture of cherry extract and 1,4-cineole was also prepared in hexane. The paper strip was then air dried for 30 s to evaporate the solvent before being placed inside one arm of the olfactometer. In the opposite arm, a filter paper loaded exclusively with hexane was used as the control stimulus.

At 15 days post-inoculation, 40 worker honey bees were used per treatment (I-DWV and N-DWV) for each evaluated stimulus. Prior to the test, each bee was acclimated within the Y-tube by placing the individual in the testing area for 5 min, followed by careful removal for 10 min; the testing area was then cleaned with 96% ethanol, following Arenas and Farina (2012).

For the test, the bee was placed in the central arm and allowed to move within the olfactometer for 6 min; a choice was recorded as the first movement into either arm of the Y-tube within that timeframe in which the insect remained for at least 30 s. The choice distribution was defined as follows: a positive choice toward the arm where the stimulus was applied, a negative choice toward the arm without the stimulus, and "no choice" when the insect failed to select either area by the end of the evaluation period. After the test, each bee was stored at -80 °C for subsequent molecular analysis. For this purpose, the expression of behavioral and glutamatergic system genes (*GLS*,

Gs2, *VGlut*, *NMDAR1*, *NMDAR2*, *Eaat1*, *Eaat2*, and *Eaat3*) was analyzed by qPCR (Table 1).

RNA Extraction, cDNA Synthesis, and Molecular Analysis

To correlate viral load with the behavioral response, total RNA extraction was performed on whole head homogenates (including antennae) derived from the bees used in both the electrophysiological response evaluation and behavioral assays. The procedure followed the methods described by Kim et al. (2019) and Silva et al. (2024) with minor modifications. The collected antennae and heads from each bioassay were homogenized with 500 µL of Trizol™ (Invitrogen, Thermo Fisher Scientific, Waltham, MA, USA) at maximum speed using a Retsch homogenizer. Subsequently, 5 µL of RNA carrier was added, following the manufacturer's recommendations (Invitrogen, Thermo Fisher Scientific). The homogenate was incubated on ice for 5 min, followed by the addition of 200 µL of chloroform and a second 3 min incubation on ice. The mixture was centrifuged for 15 min at 10,000 x g at 4 °C, and the supernatant was collected for RNA extraction.

RNA extraction was carried out using the E.Z.N.A.® Total RNA Kit I (Omega Bio-tek, Norcross, GA, USA) according to the manufacturer's instructions. RNA quality and yield were assessed using a spectrophotometer (Infinite 200 PRO NanoQuant, Tecan Group, Männedorf, Switzerland) and visualized by agarose gel electrophoresis. Then, RNA was stored at -80 °C.

For cDNA synthesis, the High Capacity cDNA Reverse Transcription Kit (Applied Biosystems, Life Technologies, Carlsbad, CA, USA) was used according to the manufacturer's protocol.

Viral quantification was performed using the cDNA synthesized from samples collected at 15 dpi. Quantitative PCR (qPCR) was conducted using the KAPA SYBR® FAST Universal 2X qPCR MasterMix (Kapa Biosystems, Wilmington, MA, USA) following the manufacturer's instructions. Reactions were set to a final volume of 15 µL, including 20 ng of cDNA, 530 µM of each primer, and sterile molecular grade filtered water. Thermal cycling conditions were optimized according to the specific requirements of each designed primer. Finally, qPCR analyses were performed using a Stratagene

Mx3000P thermocycler (Agilent Technologies, Santa Clara, CA, USA), and data were analyzed using MxPro software (Stratagene, Agilent Technologies). For viral load quantification, a standard curve was created using a purified PCR product (Wizard® SV Gel and PCR Clean Up System, Promega, Madison, WI, USA). The purified amplicon was quantified via spectrophotometry (Epoch™ Microplate Spectrophotometer, BioTek, Winooski, VT, USA), and the copy number was calculated according to Wu et al. (2017). Linear standard curves (95-100% efficiency) were generated through serial dilutions (1.0×10^{1} to 1.0×10^{9}) of the purified cDNA viral copy number. Ct values were plotted against the copy number values ($\log_{10}$). Consequently, the sample copy number was estimated using Ct values compared against the linear equation of the standard curve and normalized against the β-actin calibration values. Finally, data were expressed as the number of DWV-A copies per bee, accounting for the dilutions made during cDNA synthesis and qPCR.

The host gene expression analyses were performed using cDNA corresponding to samples collected at each bioassay, with β-actin and RPS18 used as normalization genes (Table 1). The qPCR reactions were performed using Applied Biosystems MasterMix (Thermo Fisher Scientific, Wilmington, MA, USA) in a final volume of 10 µL containing 10 ng of cDNA and 530 µM of each primer. Thermal cycling conditions were optimized for each primer pair. Reactions were run on a StepOne Real Time PCR System de Applied Biosystems (Waltham, MA 02451, USA), and data were analyzed using StepOne software.

Data Analysis

All analyses were performed in R (v. 4.5.2). Prior to analysis, missing values were excluded, and assumptions of normality and homoscedasticity were evaluated. Continuous variables failing to meet parametric assumptions (e.g., DWV-A viral load, EAG amplitudes) were compared using the Mann-Whitney *U* test, calculating the Wilcoxon effect size (r) to estimate the magnitude of differences.

To evaluate behavioral performance (coded binarily as 1=choice, 0=no choice), Generalized Linear Models (GLMs) with a binomial distribution and logit link function were constructed as a function of DWV-A load, Glutamine synthetase (*Gs2*), and

Excitatory amino acid transporter 2 (*Eaat2*) expression. Effects were reported as odds ratios (OR) with 95% CIs.

The central glutamatergic structure was explored via principal component analysis (PCA), integrating viral load and behavior as supplementary quantitative variables, and olfactory stimulus as a qualitative variable (Figures S5 and S6, Supplementary material). Bivariate associations were then assessed using Pearson correlation coefficients. Finally, the mediating role of *Eaat2* was evaluated via causal mediation analysis (counterfactual framework). Non-parametric bootstrapping (500 simulations) was used to estimate the Average Causal Mediation Effect (ACME) and Average Direct Effect (ADE). Significance was set at $p < 0.05$.

3. RESULTS

3.1. Chemical Characterization of Floral Stimuli

Characterization of the volatile fraction of blueberry revealed a composition predominantly denominated by monoterpenes, with eucalyptol as the major compound (55.09 ppm), followed by 2-carene (11.07 ppm) and α-pinene (6.50 ppm). Additionally, this fraction contained several minor compounds in concentrations below 1 ppm, notably myrcene (0.55 ppm) and farnesane (0.46 ppm) (Table 2). In contrast, the profile of cherry exhibited greater chemical diversity; although eucalyptol remained the primary compound (32.99 ppm), there was a notable contribution from sesquiterpenes (such as farnesene, 22.25 ppm) and hydrocarbons (pentadecane, 10.89 ppm). Furthermore, this profile was characterized by the presence several specific trace compounds, such as 1,3-dimethyl-2-ethylbenzene (0.44 ppm) and nonylcyclohexane (0.76 ppm) (Table 3).

3.2. Analysis of Peripheral Reception (EAG)

Electroantennographic (EAG) recordings on honey bees indicated that DWV-A infection is associated with a reduction in antennal depolarization amplitude, particularly in response to complex odors (Figure 1). Infected bees (I-DWV) exhibited significantly lower responses compared to non-inoculated bees (N-DWV) toward blueberry (I-DWV = 0.237 mV vs. N-DWV = 0.320 mV; Mann-Whitney *U* test, *p* =

0.007), cherry (I-DWV = 0.260 mV vs. N-DWV = 0.320 mV; Mann-Whitney *U* test, *p* = 0.001), and the cherry + 1,4-cineole mixture (I-DWV = 0.332 mV vs. N-DWV = 0.427 mV; Mann-Whitney *U* test, *p* = 0.002) (Figure 1). No statistical differences were detected in the response of honey bees to the isolated compound 1,4-cineole (I-DWV = 0.221 mV vs. N-DWV = 0.244 mV; Mann-Whitney U test, p = 0.188).

3.3. Molecular Analysis of Peripheral Reception

Additionally, at the peripheral level, molecular quantification of the evaluated bees confirmed that inoculated individuals (I-DWV) harbored significantly higher DWV-A viral titers compared to the basal levels of the non-inoculated control group (N-DWV) (Mann-Whitney *U* test, *p* = 0.004) (Figure S1). The expression of neuronal plasticity genes in the heads (including antennae) showed no significant variations between groups (Mann-Whitney *U* test) (Figure 2). However, a trend was observed in the relative expression of *CPeb2*, with a median value of 0.874 for the non-inoculated group compared to 1.25 for the infected group (*p* = 0.056). Similarly, *CAMKII* showed a median expression of 1.00 in the control group versus 0.714 in the DWV-A inoculated group (*p* = 0.075). The other evaluated genes did not show significant differences (*PKC*, p = 0.385; *CalpC*, *p* = 0.306; *CalpB*, *p* = 0.722).

(Figure 2). Similarly, the evaluation of genes related to glutamate homeostasis showed no statistical differences between treatments (Mann-Whitney *U* test) (Figure 3). Nevertheless, infected bees exhibited an upward trend in the relative expression of *Eaat3*, with a median value of 2.13 compared to 0.902 in the non-inoculated group (*p* = 0.104). A similar trend was observed for *Eaat2* (I-DWV median = 1.38 vs. N-DWV median = 0.799; *p* = 0.124) and *Gs2* (I-DWV median = 1.69 vs. N-DWV median = 1.07; *p* = 0.183). No notable variations were found for *Eaat1* (*p* = 0.934). (Figure 3).

3.4. Impact of DWV-A Infection on Behavioral Performance

Following the behavioral evaluations, viral quantification of the specific cohort used in these assays was performed to correlate individual infection levels with behavioral outcomes. These analyses confirmed significantly elevated DWV-A loads in the I-DWV group relative to the N-DWV controls (Mann-Whitney *U* test, *p* < 0.001) (Figure S2). In

the Y-tube olfactometer choice assays, the DWV-A load emerged as the primary predictor of behavioral impairment in honey bees. The logistic regression model revealed a significant negative association between viral titers (log_{10}) and the probability of a successful choice ($Z = -2.30$, $p = 0.022$) (Figure 4). Specifically, the model demonstrated a negative slope for viral load (Estimate = -0.3623), indicating that as the viral titer increases, the probability of the bee making a positive choice for the floral stimulus significantly decreases.

Correlation analysis revealed significant positive associations among genes associated with metabolism and signaling in the olfactory system (Figure 5). Specifically, the metabolic enzyme *GLS* showed significant correlations with *Gs2* (r = 0.68; $p < 0.001$) and the vesicular transporter *VGlut* (r = 0.54; $p < 0.001$). Furthermore, the receptor subunit *AmNMDAR2* correlated with *VGlut* (r = 0.70; $p < 0.001$) and *GLS* (r = 0.50; $p < 0.001$). Regarding excitatory amino acid transporters, *Eaat1* co-expressed with *Eaat3* (r = 0.68; $p < 0.001$) and the *AmNMDAR1* subunit (r = 0.49; $p < 0.001$). Regarding the impact of DWV-A infection, viral load showed significant positive correlations with key genes of the glutamatergic system. Most notably, it was moderately to strongly associated with the expression of the enzyme *Gs2* (r = 0.48; $p < 0.001$) and the transporter *Eaat2* (r = 0.44; $p < 0.001$), while presenting weaker but significant associations with *AmNMDAR1* (r = 0.22; $p < 0.05$) and *GLS* (r = 0.21; $p < 0.05$). Finally, when evaluating bee behavior, a significant negative correlation was identified between the behavioral choice response and viral load (r = -0.20; $p < 0.05$), indicating that higher infection levels are associated with impairment in this parameter (Figure 5).

Furthermore, given that *Eaat2* was the only gene exhibiting a positive, albeit non-significant, correlation with behavioral choice probability, a causal mediation analysis was performed to clarify the mechanism of viral action. A positive indirect effect mediated by *Eaat2* was identified (ACME > 0), in contrast to the negative direct effect of the virus (ADE < 0); consequently, the results indicate a negative total effect of high viral loads on bee behavior (Figure 6).

4. DISCUSSION

Numerous studies have evaluated the effect of DWV-A on *A. mellifera* health, focusing on systemic transcriptomic responses or the characterization of immune pathways at the whole organism level (Ray et al., 2025; Ryabov et al., 2014). However, understanding the ecological consequences of viral infection also requires evaluating vital processes such as olfaction. As generalist foragers, honey bees rely on an efficient ability to discriminate and learn complex olfactory signals for survival (Pizzorno et al., 2021). The decoding of these ecologically relevant odors demands coordination between peripheral sensory transduction and integrative processing in the brain (Carcaud et al., 2015; Galizia & Rossler, 2010).

To determine whether the olfactory deficit induced by DWV-A originates in the sensory periphery or through a breakdown in central neurotransmission, this study analyzed transcriptional alterations along the olfactory circuit of A. mellifera after exposure to complex olfactory stimuli such as the volatile fraction of blueberry and cherry flowers, and simple stimuli such as a pure terpene, 1,4-cineole. Increased DWV-A viral load significantly reduced peripheral detection capacity, as reflected in the decreased electroantenographic amplitude in bees with high viral loads exposed to the different stimuli. This phenotype has been previously described as a direct consequence of increased viral loads in the sensory structures of bees when exposed to other stimuli (Silva et al., 2025; Silva et al., 2021) and has been suggested to be caused by damage to the cellular ultrastructure occurring in the vicinity of peripheral nervous system cells (Kim et al., 2019). This suggests that the virus interferes with the integrity of the peripheral nervous system, causing this change in the anatomical conformity of the epithelial tissue to compromise the metabolic functionality of nearby cells, since Kim et al. (2019) demonstrated that the damage to the cellular ultrastructure was characterized by constant viral replication in epithelial cells.

Although the evaluation of the genes analyzed in the electrophysiological assay did not show strict statistical significance, the expression profiles revealed trends between the treatment of bees inoculated with DWV-A (I-DWV) and uninoculated bees (N-DWV). These alterations could be biologically relevant, particularly the trends observed in the Gs2, Eaat2, and Eaat3 genes. However, in the behavioral assays,

when analyzing individual bees, the gene expression in the different treatments for these same genes significantly confirmed the difference in expression between treatments with high and low viral loads. In the correlation analysis, it was confirmed that the overexpression of the Gs2 and Eaat2 genes was positively associated with increased viral loads, confirming that these genes responded directly to the pathogen. The dysregulation of Gs2 by DWV has been described by Chen et al. (2021), who postulate that alteration of this gene would deregulate glutamate levels and that, consequently, the imbalance of this neurotransmitter would alter the learning and behavioral processes of bees. While the reports by Chen et al. (2021) link the virus to glutamate regulation through the suppression of Gs2-like genes, it is possible to relate the overexpression detected in this study to the increased viral load of DWV-A, based on recent evidence that impacts high viral replication rates with profound systemic metabolic stress.

As reported by Ray et al. (2025), high viral loads of DWV-A induce host reprogramming towards aerobic glycolysis, a phenomenon analogous to the "Warburg Effect" that favors rapid viral replication and leads to a direct increase in brain glutamate production. While the studies reported by Chen et al. (2021) initially reported that Gs2 gene expression was suppressed by increased viral loads. They observed an increase in glutamine concentration in the brains of bees, compared to glutamate concentration. This demonstrates that even when Gs2 gene expression was low, enzymatic activity was significantly higher. In contrast, Traniello et al. (2020) demonstrated that, at the cellular level, increased viral loads under asymptomatic conditions increase the number of glial cells in infected nurse bees, under conditions similar to those of our study. They also observed an increase in canonical glial markers, including the Gs2 gene. Consequently, while the reports by Chen et al. (2021) and Traniello et al. (2020) show different changes in Gs2 gene expression in response to viral load, suggesting that glial activity, in particular, is sensitive to increased DWV-A viral loads, potentially compromising the metabolic regulation of this cell group.Furthermore, the taurine/aspartate transporter *Eaat-2* has been described as the functional ortholog of mammalian glutamate transporters in insects (Besson et al., 1999), and in the model organism *D. melanogaster* it has been described in glial

cells, of the central nervous system during larval stages (Soustelle et al., 2002). In this sense, in *D. melanogaster*, the silencing of *Eaat2* expression in antennal glial cells, generated behavioral alterations, due to changes in olfactory sensitivity, postulating it as a regulator of the activity of sensory olfactory neurons (OSNs) (Calvin-Cejudo et al., 2023). Additionally, the overexpression of transporters such as Eaat2 has been previously reported using RNA-seq assays by Rittschof and Schirmeier (2018) and Silva et al. (2026), and has been proposed as a possible homeostatic response linked to glutamate levels and cellular stress.

Although glutamate levels were not determined in this study, based on reports for the Gs2 and Eaat2 genes, along with the relationship of DWV to increased glutamate levels assessed by Chen et al. (2021), we postulate that the nervous system may hyperactivate its enzymatic recycling (Gs2) and reuptake pathways, including Eaat2, along with other potentially involved glial and neuronal transporters, to clear excess glutamate derived from viral metabolic sequestration proposed by Ray et al. (2025). Additionally, recent studies have observed that increased viral loads induce an increase in metabolic stress regulators, including glutamate regulators, linking the metabolic flux proposed by Ray et al. (2025) and a cellular response associated with glutamate stress (Silva et al., 2026). It has been proposed that a biphasic response in the central nervous system occurs during DWV-A infection (Silva et al. 2026). Specifically, an early and transient upregulation of key genes in the glutamatergic network, including the Eaat-2, Neto, and Kainate receptors, was revealed. This is postulated as a homeostatic attempt to remove excess glutamate from the synaptic cleft via ATP-dependent active transport. However, as viral replication pressure increases, the high energy cost of maintaining this removal becomes unsustainable, ultimately leading to the collapse of the regulatory network and severe synaptic dysregulation.

The positive association observed between Gs2 and Eaat2 expression levels and increased viral load suggests a complex molecular response that goes beyond direct cell damage. While previous studies by Ray et al. (2025) and Silva et al. (2026) are a recent approach to this phenomenon, they have suggested that DWV-A generates metabolic stress by altering glutamate homeostasis. Thus, the results of this study

further link increased viral loads to a much more complex phenomenon previously described.

Traniello et al. (2020) proposed that high viral loads in asymptomatic bees induce accelerated premature development, leading to foraging deficiencies, mainly due to a marked increase in the expression of regulators of bee physiological maturation, primarily those of the transcription factor owo, and an increase in canonical glial cell markers such as Repo and Gs2. Interestingly, similar to our study, Repo and Gs2 showed positive correlations and greater overexpression in all bees with high DWV-A viral loads, suggesting a pathogen-induced increase in the number of glial cells (Traniello et al., 2020). Additionally, the association between Gs2 and bee maturation was recently confirmed by Mu et al. (2025), who indicated that this gene was overexpressed under normal conditions precisely during the transition from nurse to forager bees. Furthermore, Ferreira et al. (2025) reported that bees with high DWV-A viral loads begin collecting nectar earlier than expected compared to bees from hives with low viral loads, which are characterized by poor nectar and foraging performance. On the other hand, the dysregulation of bee maturation as a consequence of viral increase was observed in the study by Silva et al. (2026), who, like Traniello et al. (2020), identified an increase in the transcription factor owo in bees inoculated with DWV-A. This suggests that this phenomenon of premature maturation is not an isolated effect, but rather a phenomenon that has not yet been fully characterized. In general, and analyzing the results presented in our work, although Gs2 did not correlate significantly with the observed behavioral responses, it did correlate positively with the increase in viral loads, potentially being an indicator of the molecular alterations induced by the pathogen, rather than a response directly associated with the behavioral alteration.

The viral load induced sensory collapse, observed in our regression and mediation models, is consistent with the marked behavioral impairment recently reported by Silva et al. (2025). These authors demonstrated that high DWV-A viral loads significantly reduce bee attraction toward various pollen scents, including polyfloral pollen compared to monofloral pollen from *Rubus ulmifolius* and *Eucryphia cordifolia*, with this deficit manifesting severely and sustainably starting at 10 days post-infection (dpi). Given that the physiological and behavioral evaluations in the present study were

conducted at 15 dpi, our results precisely evidence a stage of maximum neurobiological deterioration. This chronological progression fully aligns with our predictive model, suggesting that the disruption of decision making is not an acute response to the onset of infection (low viral loads), but rather the consequence of a cumulative degenerative process associated with rising viral titers.

In summary, the olfactory and behavioral deficits induced by the Deformed Wing Virus variant A (DWV-A) in *A. mellifera* result from an asymmetric mechanism within its sensory circuit. At the peripheral level, the infection significantly reduces the amplitude of electroantennogram responses to complex chemical stimuli, independent of the antennal expression of glutamatergic or plasticity related genes. The molecular impact is concentrated in the central nervous system, where increased viral load acts as a direct predictor of impaired behavioral choice and induces coordinated overexpression of the *Gs2* enzyme and the transporter *Eaat2*. Causal mediation analysis quantifies this dynamic, demonstrating that while viral replication has a direct negative effect on performance, the upregulation of *Eaat2* has an indirect positive effect. This provides mechanistic evidence that the increase in glial network gene expression is not the result of transcriptional depletion, but rather a compensatory response aimed at stabilizing glutamate levels through reuptake mechanism; these mechanisms, however, proves insufficient in the face of high pathogen replication rates, ultimately leading to impaired odor discrimination by honey bees.

Acknowledgments: F.B. wishes to express his gratitude for the support of his master's studies through the FONDECYT project N°. 1241994. The authors would like to express their gratitude to the Master's Program in Agronomic Sciences at the University of Concepción (Chile).

Author Contributions: Conceptualization: M.V., C.G-D., D.S.; Methodology: M.V., C.G-D., D.S., R.C.; Formal analysis: F.B., D.S.; Investigation: F.B., Y.F., D.V., D.S.,Writing original draft: F.B., Writing review & editing: M.V., C.G-D., F.B., D.S., Y.F., D.V., N.A., R.C. Supervision: M.V., D.S., Project administration: M.V., Funding acquisition: M.V., Resources: M.V., All authors have read and agreed to the published version of the manuscript.

Funding: This study was funded within the framework of FONDECYT project N° 1241994 and 1240089, supported by the National Research and Development Agency (ANID), Chile.

Declarations

Competing interests: The authors declare no competing interests. Correspondence and requests for materials should be addressed to M.V.

REFERENCES

Arenas, A., and Farina, W. M. (2012). Learned olfactory cues affect pollen-foraging preferences in honeybees, *Apis mellifera*. Anim. Behav. 83, 1023-1033. doi: 10.1016/j.anbehav.2012.01.026

Arismendi, N., Caro, S., Castro, M. P., Vargas, M., Riveros, G., and Venegas, T. (2020). Impact of Mixed Infections of gut parasites *Lotmaria passim* and *Nosema ceranae* on the lifespan and immune-related Biomarkers in *Apis mellifera*. Insects 11:420. doi: 10.3390/insects11070420

Basualdo, M., Cavigliasso, P., de Avila, R. S., Aldea-Sánchez, P., Correa-Benítez, A., Harms, J. M., et al. (2022). Current status and economic value of insect-pollinated dependent crops in Latin America. Ecol. Econ. 196:107395. doi: 10.1016/j.ecolecon.2022.107395

Besson, M. T., Soustelle, L., and Birman, S. (1999). Identification and structural characterization of two genes encoding glutamate transporter homologues differently expressed in the nervous system of *Drosophila melanogaster*. FEBS Lett. 443, 97-104. doi: 10.1016/s0014-5793(98)01695-0

Calvin-Cejudo, L., Martin, F., Mendez, L. R., Coya, R., Castaneda-Sampedro, A., Gomez-Diaz, C., et al. (2023). Neuron-glia interaction at the receptor level affects olfactory perception in adult *Drosophila*. iScience 26:105837. doi: 10.1016/j.isci.2022.105837

Carcaud, J., Giurfa, M., and Sandoz, J. C. (2015). Parallel Olfactory Processing in the Honey Bee Brain: Odor Learning and Generalization under Selective Lesion of a Projection Neuron Tract. Front. Integr. Neurosci. 9:75. doi: 10.3389/fnint.2015.00075

Chen, P., Lu, Y. H., Lin, Y. H., Wu, C. P., Tang, C. K., Wei, S. C., et al. (2021). Deformed wing virus infection affects the neurological function of *Apis mellifera* by altering extracellular adenosine signaling. Insect Biochem. Mol. Biol. 139:103674. doi: 10.1016/j.ibmb.2021.103674

Cook, S. M., Sandoz, J.-C., Martin, A. P., Murray, D. A., Poppy, G. M., and Williams, I. H. (2005). Could learning of pollen odours by honey bees (*Apis mellifera*) play a role in their foraging behaviour? Physiol. Entomol. 30, 164-174. doi: 10.1111/j.1365-3032.2005.00445.x

de Miranda, J. R., Bailey, L., Ball, B. V., Blanchard, P., Budge, G. E., Chejanovsky, N., et al. (2015). Standard methods for virus research in *Apis mellifera*. J. Apic. Res. 52, 1-56. doi: 10.3896/ibra.1.52.4.22

Ferreira, H. M., Benaets, K., De Smet, L., de Graaf, D. C., and Wenseleers, T. (2025). Deformed wing virus affects foraging success and foraging specialization of honeybee workers. Sci. Rep. 16:2029. doi: 10.1038/s41598-025-31753-0

Galizia, C. G., and Rossler, W. (2010). Parallel olfactory systems in insects: anatomy and function. Annu. Rev. Entomol. 55, 399-420. doi: 10.1146/annurev-ento-112408-085442

Gusachenko, O. N., Woodford, L., Balbirnie-Cumming, K., Ryabov, E. V., and Evans, D. J. (2020). Evidence for and against deformed wing virus spillover from honey bees to bumble bees: a reverse genetic analysis. Sci. Rep. 10:16847. doi: 10.1038/s41598-020-73809-3

Hsieh, E. M., Carrillo-Tripp, J., and Dolezal, A. G. (2020). Preparation of virus-enriched inoculum for oral infection of honey bees (*Apis mellifera*). J. Vis. Exp. 162:e61725.

Kim, S. H., Mercer, A., Mitchell, A., de Miranda, J. R., Ward, V., Mondet, F., et al. (2019). Viral infections alter antennal epithelium ultrastructure in honey bees. J. Invertebr. Pathol. 168:107252. doi: 10.1016/j.jip.2019.107252

Kucharski, R., Ball, E. E., Hayward, D. C., and Maleszka, R. (2000). Molecular cloning and expression analysis of a cDNA encoding a glutamate transporter in the honeybee brain. Gene 242, 399-405. doi: 10.1016/S0378-1119(99)00503-X

Liu, W. W., and Wilson, R. I. (2013). Glutamate is an inhibitory neurotransmitter in the *Drosophila* olfactory system. Proc. Natl. Acad. Sci. U.S.A. 110, 10294-10299. doi: 10.1073/pnas.1220560110

Martin, S. J., and Brettell, L. E. (2019). Deformed Wing Virus in Honeybees and Other Insects. Annu. Rev. Virol. 6, 49-69. doi: 10.1146/annurev-virology-092818-015700

Mateos-Fierro, Z., Garratt, M. P. D., Fountain, M. T., Ashbrook, K., and Westbury, D. B. (2025). Contribution of pollinators to delivering fruit quality in commercial sweet cherry orchards. JSFA Rep. 5, 330-336. doi: 10.1002/jsf2.70012

Menzel, R. (2012). The honeybee as a model for understanding the basis of cognition. Nat. Rev. Neurosci. 13, 758-768. doi: 10.1038/nrn3357

Mu, X., Zhang, Z., Liu, Q., Ma, J., Qin, Y., Lang, H., et al. (2025). Single-nucleus and spatial transcriptomics identify brain landscape of gene regulatory networks associated with behavioral maturation in honeybees. Nat. Commun. 16:3343. doi: 10.1038/s41467-025-58614-8

Paoli, M., and Galizia, G. C. (2021). Olfactory coding in honeybees. Cell Tissue Res. 383, 35-58. doi: 10.1007/s00441-020-03385-5

Paxton, R. J., Schafer, M. O., Nazzi, F., Zanni, V., Annoscia, D., Marroni, F., et al. (2022). Epidemiology of a major honey bee pathogen, deformed wing virus: potential worldwide replacement of genotype A by genotype B. Int. J. Parasitol. Parasites Wildl. 18, 157-171. doi: 10.1016/j.ijppaw.2022.04.013

Pizzorno, M. C., Field, K., Kobokovich, A. L., Martin, P. L., Gupta, R. A., Mammone, R., et al. (2021). Transcriptomic Responses of the Honey Bee Brain to Infection with Deformed Wing Virus. Viruses 13:287. doi: 10.3390/v13020287

Ray, A. M., Tehel, A., Rasgon, J. L., Paxton, R. J., and Grozinger, C. M. (2025). The intensity of the transcriptional response varies across infection with distinct viral strains in an insect host. BMC Genomics 26:175. doi: 10.1186/s12864-025-11365-8

Reilly, J. R., Artz, D. R., Biddinger, D., Bobiwash, K., Boyle, N. K., Brittain, C., et al. (2020). Crop production in the USA is frequently limited by a lack of pollinators. Proc. Biol. Sci. 287:20200922. doi: 10.1098/rspb.2020.0922

Rittschof, C. C., and Schirmeier, S. (2018). Insect models of central nervous system energy metabolism and its links to behavior. Glia 66, 1160-1175. doi: 10.1002/glia.23235

Riveros, G., Arismendi, N., Zapata, N., Evans, D., Pérez, I., Aldea, P., et al. (2019). Occurrence, prevalence and viral load of deformed wing virus variants in *Apis mellifera* colonies in Chile. J. Apic. Res. 59, 1-6. doi: 10.1080/00218839.2019.1670993

Ryabov, E. V., Wood, G. R., Fannon, J. M., Moore, J. D., Bull, J. C., Chandler, D., et al. (2014). A virulent strain of deformed wing virus (DWV) of honeybees (*Apis mellifera*) prevails after *Varroa destructor*-mediated, or in vitro, transmission. PLoS Pathog. 10:e1004230. doi: 10.1371/journal.ppat.1004230

Schwaerzel, M., Monastirioti, M., Scholz, H., Friggi-Grelin, F., Birman, S., and Heisenberg, M. (2003). Dopamine and octopamine differentiate between aversive and appetitive olfactory memories in *Drosophila*. J. Neurosci. 23, 10495-10502.

Shah, A. K., Kreibich, C. D., Amdam, G. V., and Munch, D. (2018). Metabolic enzymes in glial cells of the honeybee brain and their associations with aging, starvation and food response. PLoS One 13:e0198322. doi: 10.1371/journal.pone.0198322

Shah, K. S., Evans, E. C., and Pizzorno, M. C. (2009). Localization of deformed wing virus (DWV) in the brains of the honeybee, *Apis mellifera* Linnaeus. Virol. J. 6:182. doi: 10.1186/1743-422x-6-182

Silva, Traverso, L., Dominguez, G., Becerra, F., Fuentes, Y., Ons, S., et al. (2026). Differential expression of neuronal function genes follows a tissue-specific temporal dynamic during Deformed Wing Virus infection in honey bees. Sci. Rep. doi: 10.1038/s41598-026-57691-z

Silva, D., Arismendi, N., Pablo, A. J., Ceballos, R., Zapata, N., and Vargas, M. (2024). Nursing Honeybee Behavior and Sensorial-Related Genes Are Altered by Deformed Wing Virus Variant A. Insects 15:80. doi: 10.3390/insects15020080

Silva, D., Becerra, F., Salazar, S., Arismendi, N., Alveal, J. P., Ceballos, R., et al. (2025). Deformed wing virus–induced changes in honey bee reception and preference for pollen scents. Apidologie 56. doi: 10.1007/s13592-025-01196-7

Silva, D., Ceballos, R., Arismendi, N., Dalmon, A., and Vargas, M. (2021). Variant A of the Deformed Wings Virus Alters the Olfactory Sensitivity and the Expression of Odorant Binding Proteins on Antennas of *Apis mellifera*. Insects 12:895. doi: 10.3390/insects12100895

Soustelle, L., Besson, M. T., Rival, T., and Birman, S. (2002). Terminal glial differentiation involves regulated expression of the excitatory amino acid transporters in the *Drosophila* embryonic CNS. Dev. Biol. 248, 294-306. doi: 10.1006/dbio.2002.0742

Traniello, I. M., Bukhari, S. A., Kevill, J., Ahmed, A. C., Hamilton, A. R., Naeger, N. L., et al. (2020). Meta-analysis of honey bee neurogenomic response links Deformed wing virus type A to precocious behavioral maturation. Sci. Rep. 10:3101. doi: 10.1038/s41598-020-59808-4

Vargas, M., Arismendi, N., Riveros, G., Zapata, N., Bruna, A., Vidal, M., et al. (2017). Viral and intestinal diseases detected in *Apis mellifera* in Central and Southern Chile. Chil. J. Agric. Res. 77, 243-249. doi: 10.4067/s0718-58392017000300243

Wright, G. A., Skinner, B. D., and Smith, B. H. (2002). Ability of honeybee, *Apis mellifera*, to detect and discriminate odors of varieties of canola (*Brassica rapa* and *Brassica napus*) and snapdragon flowers (*Antirrhinum majus*). J. Chem. Ecol. 28, 721-740.

Wu, Y., Dong, X., and Kadowaki, T. (2017). Characterization of the Copy Number and Variants of Deformed Wing Virus (DWV) in the Pairs of Honey Bee Pupa and Infesting *Varroa destructor* or *Tropilaelaps mercedesae*. Front. Microbiol. 8:1558. doi: 10.3389/fmicb.2017.01558

Xia, S., Miyashita, T., Fu, T.-F., Lin, W.-Y., Wu, C.-L., Pyzocha, L., et al. (2005). NMDA receptors mediate olfactory learning and memory in *Drosophila*. Curr. Biol. 15, 603-615.

TABLES AND FIGURES

Table 1. Primer sequences designed for gene expression analysis using real-time quantitative PCR (qPCR), including DWV, reference genes, and genes of interest.

Primer		Sequence (5′–3′)	Target	Reference
GAPDH	F	CACCTTCTGCAAAATTATGGCG	Glyceraldehyde-3-phosphate dehydrogenase	(Deng et al., 2020)
	R	ACCTTTGCCAAGTCTAACTGTTAA		
RPS18	F	GATTCCCGATTGGTTTTTGAATAG	Ribosomal protein S18	(Deng et al., 2020)
	R	AACCCCAATAATGACGCAAACC		
DWV-A	F	CTGTATGTGGTGTGCCTGGT	Deformed Wing Virus Type A	(Yang & Cox, 2005)
	R	TTCAAACAATCCGTGAATATAGTGT		
CamKII	F	AACACGAAAAAGCTCACCGC	Ca2+/calmodulin-dependent protein kinase II	This study
	R	CGCCACGATATCCTCGAACA		
PKC	F	TTCCTGGTCCAACTGCACTC	Protein kinase C	This study
	R	TCGGACGCGTAGAATACAGC		
Cpeb2	F	TCCAGGAAAGTGTTCGTCGG	Cytoplasmic polyadenylation element-binding protein 2	This study
	R	AAGCAAGAAAGCGTAGCCCT		
CalpB	F	ACGTTCAGCAGGGCGAATTA	Calpain-B	This study
	R	CCACGTCTACCCATCTACCG		
CalpC	F	TCCTCTTGGACCTGGTAGGG	Calpain-C	This study
	R	TCATCCCTCGACGTTTCAGC		
GLS	F	GAGGTTCAGCATCGGTGACA	Glutaminase	This study
	R	TCAGAGGCTTGCTGCAACTTT		
*Gln*s	F	AGCAAACAACACCTAAGGCACAT	Glutamine synthetase	This study
	R	CGTCGCTCGTTGTCTTTTCC		
VGlut	F	TGATCAACAACCCGTGGACA	Vesicular glutamate transporter	This study
	R	GTCCAATTAGTTGAAGGATCGATGA		
NMDAR1	F	GTTTAGCAGTCGATACGGTAGC	NMDA receptor subunit 1	This study
	R	ATGAGATGTGAGACGTTTGCTG		
NMDAR2	F	ATGCACACGTACATGAAGGAGT	NMDA receptor subunit 2	This study
	R	CCGTCATCCAATACCTCCTCAG		
EaaT-1	F	CCACGAGAGAAATCGGTGCT	Excitatory amino acid transporter	This study

	R	AGGTCGAGAGGCTGAAAACG	1	
EaaT-2	F	GCAGGCGCAAACTACTTACG	Excitatory amino acid transporter	
	R	CATGCCCATCACATTCGTCC	2	This study
EaaT-3	F	GGACGTATAGCCGGAGTTCG	Excitatory amino acid transporter	
	R	AGAACAGAGCCCTTCGCATC	3	This study

Table 2. Composition of floral volatile emissions and concentration (ppm) of the identified compounds in blueberries (*Vaccinium corymbosum* L.).

Volatile fraction blueberry (*Vaccinium corymbosum*)		
RT	**Compound name**	**Concentration (ppm)**
10.80	α-Thujene	1.15
11.01	α-Pinene	6.50
11.75	(+)-Sabinene	1.69
11.88	β-Pinene	1.16
11.95	Myrcene	0.55
12.35	α-Phellandrene	1.00
13.01	Eucalyptol	55.09
13.35	γ-Terpinene	1.20
13.95	2-Carene	11.07
15.43	IS (Tetraline)	10.00
17.30	Tridecane	0.82
18.50	Farnesane	0.46
18,83	Tetradecane	2.26
19.09	β-Bourbonene	0.61
19.67	Bicyclo[7.2.0] undec-4-ene, 4,11,11-trimethyl-8-methylene-, (Z)-	1.02
19.74	2-Methyl-6-propyldodecane	1.92
19.86	3-Methyltetradecane	0.57
20.26	Pentadecane	4.74
20.51	Germacrene D	1.53
21.11	2,6,10-Trimethyltetradecane	0.51
21.59	Hexadecane	2.47
22.22	2,6,10-Trimethylpentadecane	0.66
22.85	Heptadecane	0.98
22.94	Pristane	0.78

Table 3. Composition of floral volatile emissions and concentration (ppm) of the identified compounds in wild cherry (*Prunus avium* L).

Volatile fraction cherry (*Prunus avium)*		
RT	**Compound name**	**Concentration (ppm)**
11.00	α-Pinene	5.23
11.87	β-Pinene	1.07
12.72	1,3-Dimethyl-2-ethylbenzene	0.44
12.98	Eucalyptol	32.99
15.43	IS (Tetraline)	10.00
17.30	Tridecane	0.87
18.49	Farnesan	0.57
18.83	Tetradecane n-Tetradecane	3.51
19.74	2-Methyl-6-propyldodecane	3.62
20.30	Pentadecane	10.89
20.51	Farnesene	22.25
20.88	7-Methylpentadecane	1.06
21.11	2,6,10-Trimethyltetradecane	1.16
21.16	Nonylcyclohexane	0.76
21.60	Hexadecane	5.74
22.22	2,6,10-Trimethylpentadecane	1.51
22.84	Heptadecane	2.12
22.93	Pristane	1.40

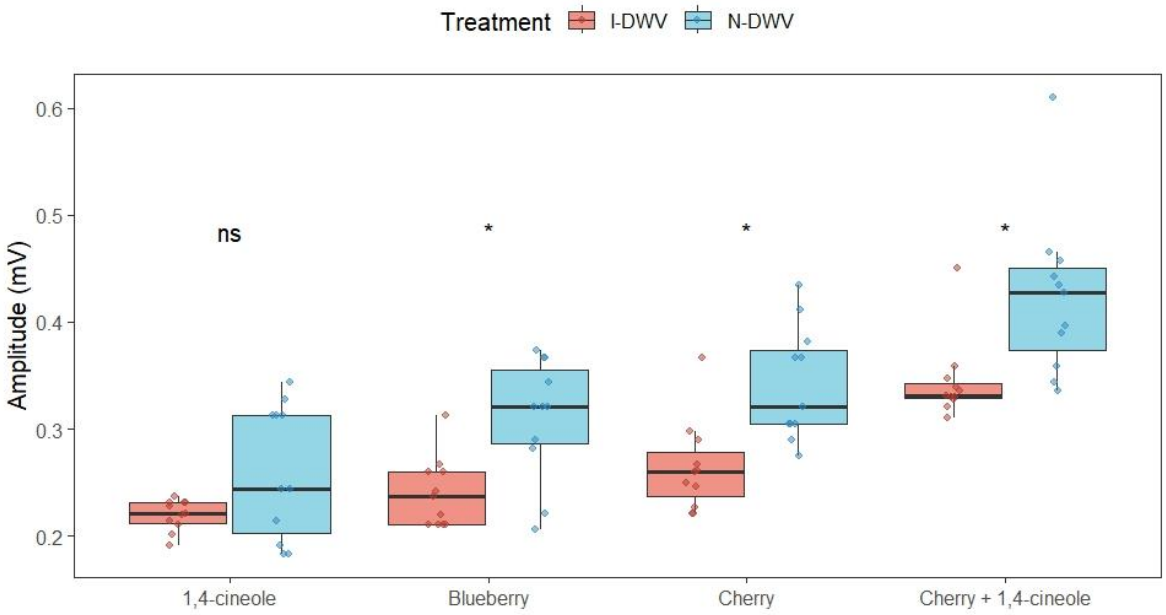

Figure 1. Amplitude of electroantennographic responses (mV) to different olfactory stimuli in *A. mellifera* inoculated and non-inoculated with DWV-A. Four stimuli were evaluated: 1,4-cineole, blueberry, cherry, and a mixture of cherry + 1,4-cineole. The box plots show the data distribution for DWV-inoculated bees (I-DWV, red; n = 5) and non-inoculated bees (N-DWV, blue; n = 5). Boxes indicate median and 25th-75th percentiles; whiskers extend to 1.5×IQR. Differences between treatments for each stimulus were assessed using the Mann-Whitney *U* test ($p < 0.05$; ns: not significant).

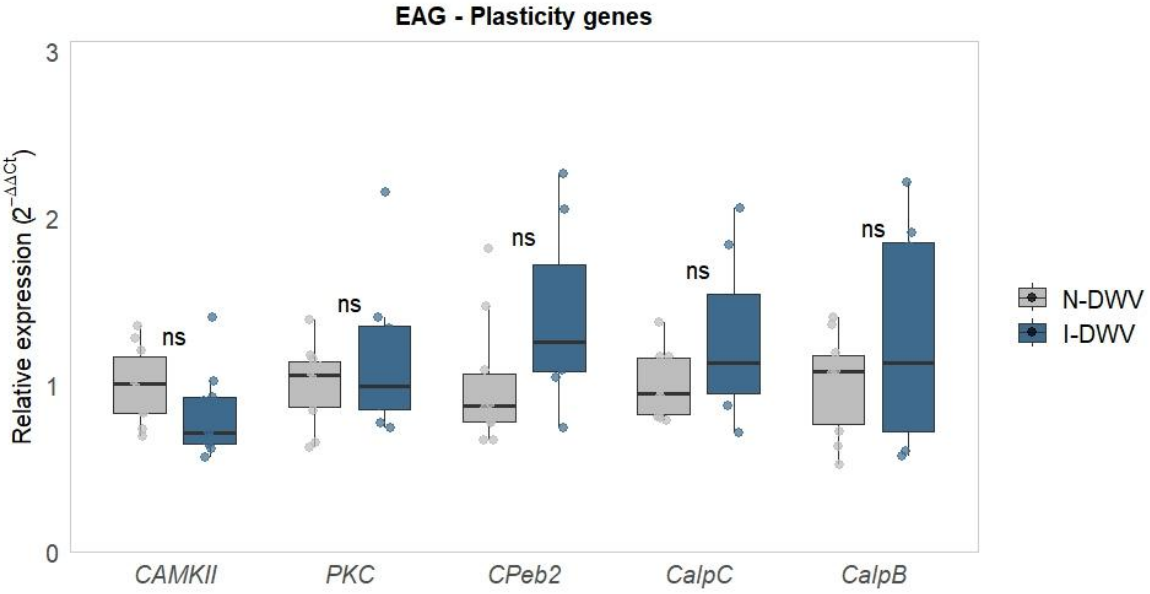

Figure 2. Relative expression of genes associated with neuronal plasticity (*CAMKII*, *PKC*, *CPeb2*, *CalpC*, and *CalpB*) in *A. mellifera* whole heads (including antennae) following olfactory stimulation (EAG). The box plots show the relative expression ($2^{-\Delta\Delta Ct}$) for DWV-A inoculated bees (I-DWV, blue; n = 5) and non-inoculated bees (N-DWV, gray; n = 5). Boxes indicate the median and 25th-75th percentiles; whiskers extend to 1.5 times the interquartile range (IQR). Dots represent individual data points. Differences between treatments for each gene were assessed using the Mann-Whitney *U* test ($p < 0.05$; ns: not significant).

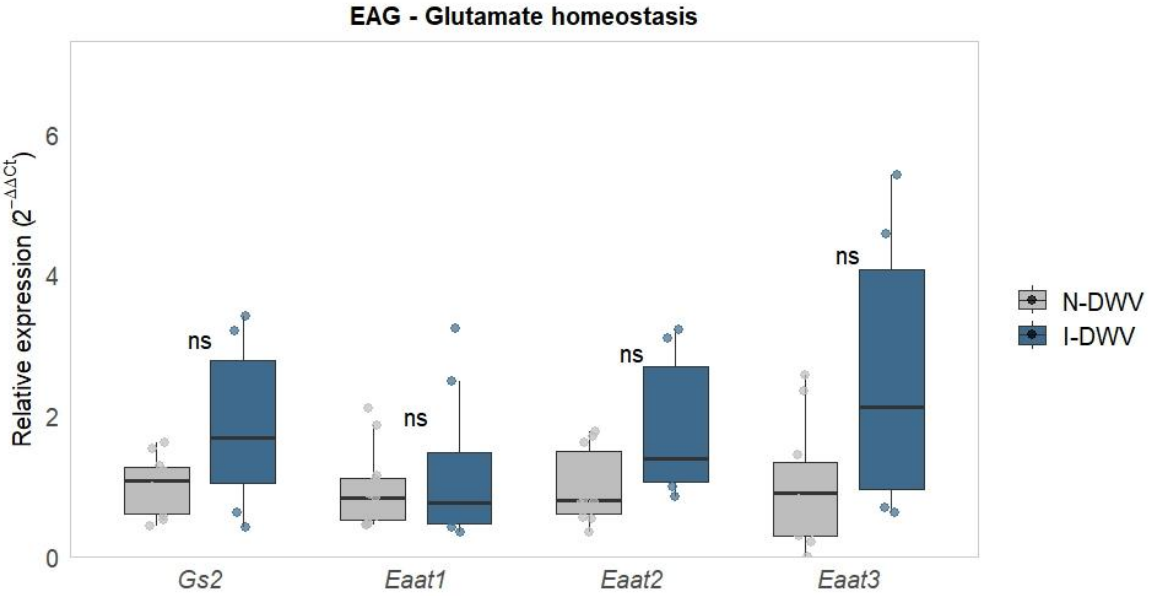

Figure 3. Relative expression of genes associated with glutamate homeostasis (*Gs2*, *Eaat1*, *Eaat2*, *Eaat3*) in *A. mellifera* whole heads (including antennae) (EAG). The box plots show the relative expression ($2^{-\Delta\Delta Ct}$) for DWV-A inoculated bees (I-DWV, blue; n = 5) and non-inoculated bees (N-DWV, gray; n = 5). Boxes indicate the median and 25th-75th percentiles; whiskers extend to 1.5 times the interquartile range (IQR). Dots represent individual data points. Differences between treatments for each gene were assessed using the Mann-Whitney *U* test ($p < 0.05$; ns: not significant).

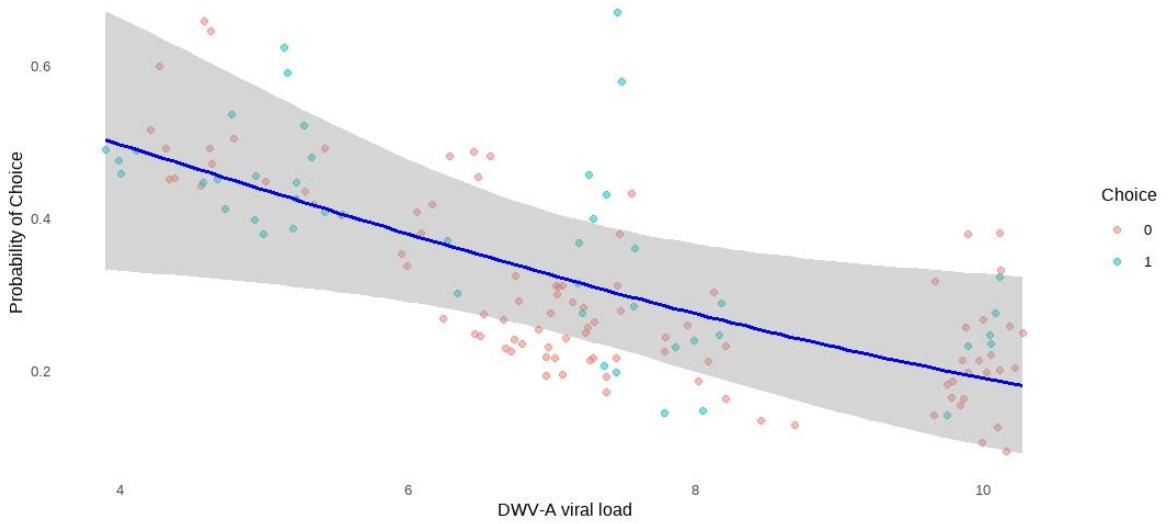

Figure 4. Probability of *A. mellifera* choosing the floral stimuli (cherry, blueberry, or a mixture of cherry + 1,4-cineole) in a Y-tube olfactometer as a function of DWV-A viral load. Data from the three independent olfactory assays were pooled to evaluate the overall effect of viral load on behavioral choice. The blue line represents the logistic regression model fitted between viral load (log_{10}) and choice. The data points correspond to individual observations (1 = choosing a floral stimulus, n = 46; 0 = no choice or choosing the control, n = 96). The shaded area indicates the 95% confidence interval.

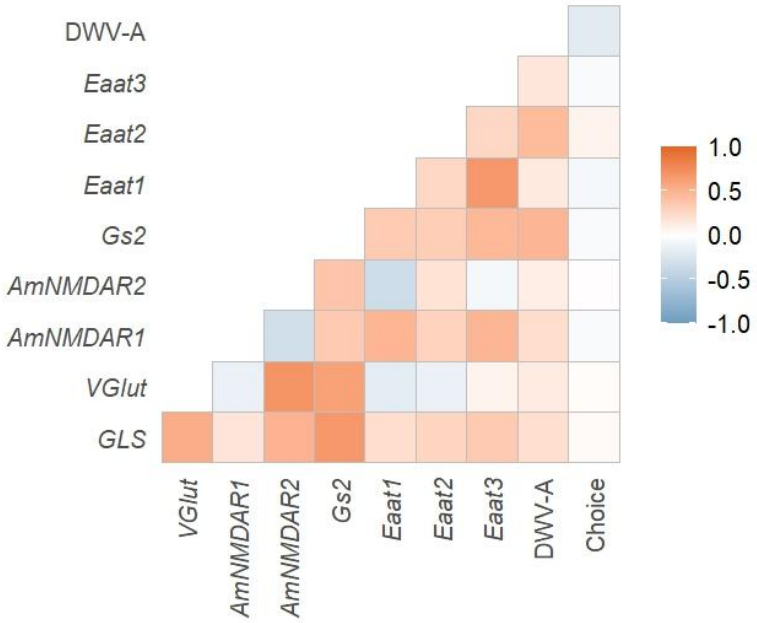

Figure 5. Pearson correlation matrix showing the relationship between gene expression in the glutamatergic system, DWV-A viral load, and behavioral response in *A. mellifera*. The color scale represents the correlation coefficient (r), with orange indicating positive associations and blue indicating negative associations.

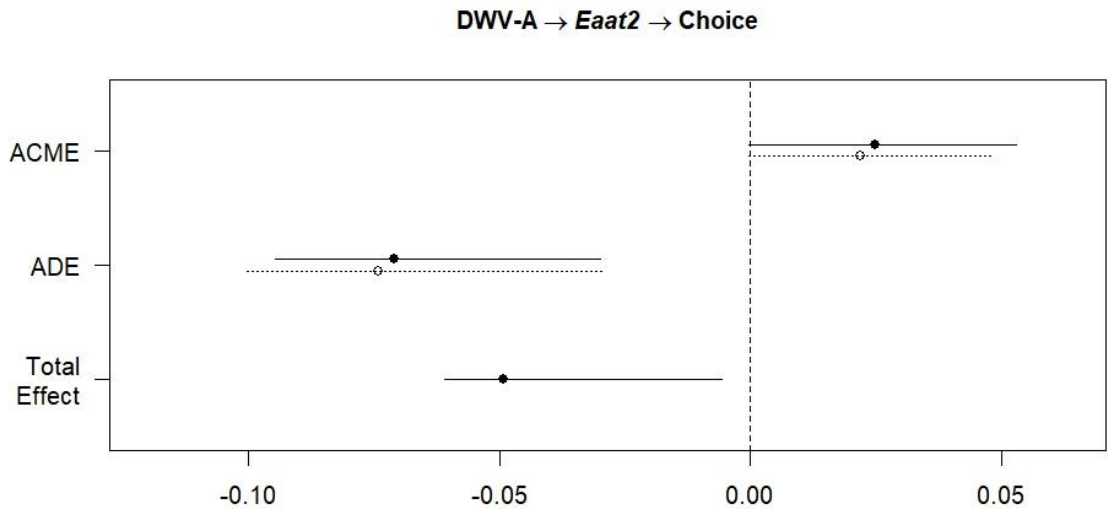

Figure 6. Causal mediation analysis of the effect of DWV-A on behavior response by *Eaat2*. Point estimates and 95% confidence intervals are shown for the average causal mediated effect (ACME), the average direct effect (ADE), and the total effect. The dashed vertical line indicates the null effect point (0.00); estimates whose intervals exclude this value indicate statistical significance ($p < 0.05$). Solid symbols represent effect estimates under the treatment condition (T=1), while open symbols indicate estimates under the control condition (T=0) in the mediation model. Inference was performed using nonparametric bootstrapping with 500 simulations.

SUPPLEMENTARY MATERIAL

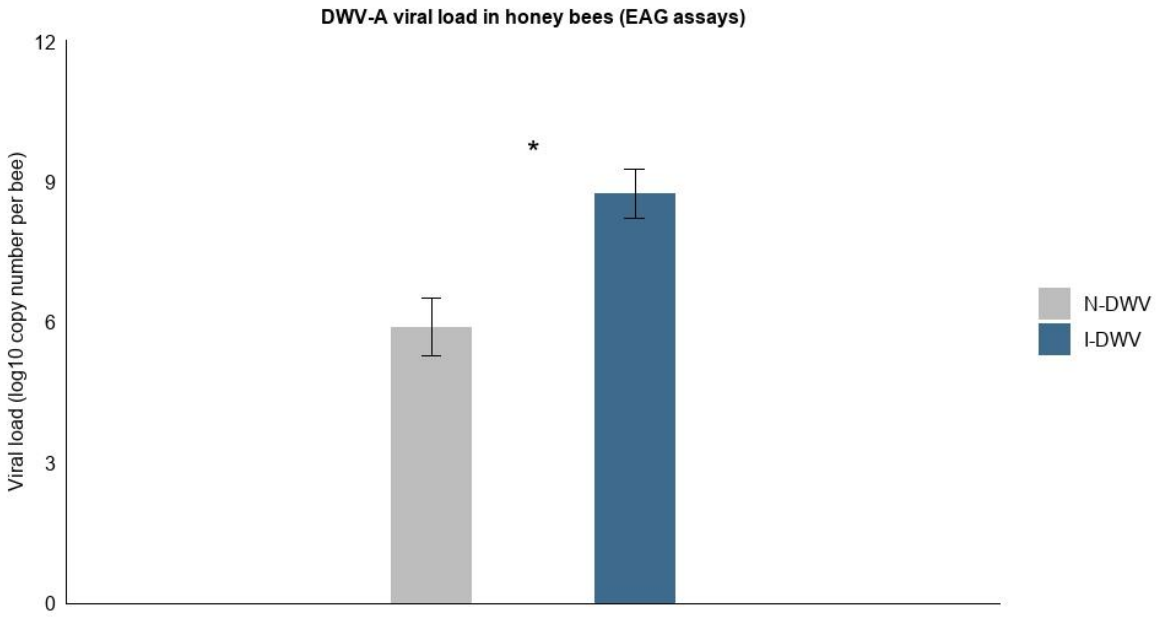

Figure S1. Quantification of DWV-A viral load in *A. mellifera* whole heads (including antennae) from individuals previously subjected to electroantennography (EAG). Bars represent the absolute viral load (log_{10} copies/bee) at 15 days post-infection (dpi) of individuals inoculated (I-DWV) non-inoculated (N-DWV) with Deformed Wing Virus variant A (DWV-A). Error bars indicate the standard error of the mean (SEM). The asterisk (*) denotes statistically significant differences between treatments ($p < 0.05$, Mann-Whitney *U* test).

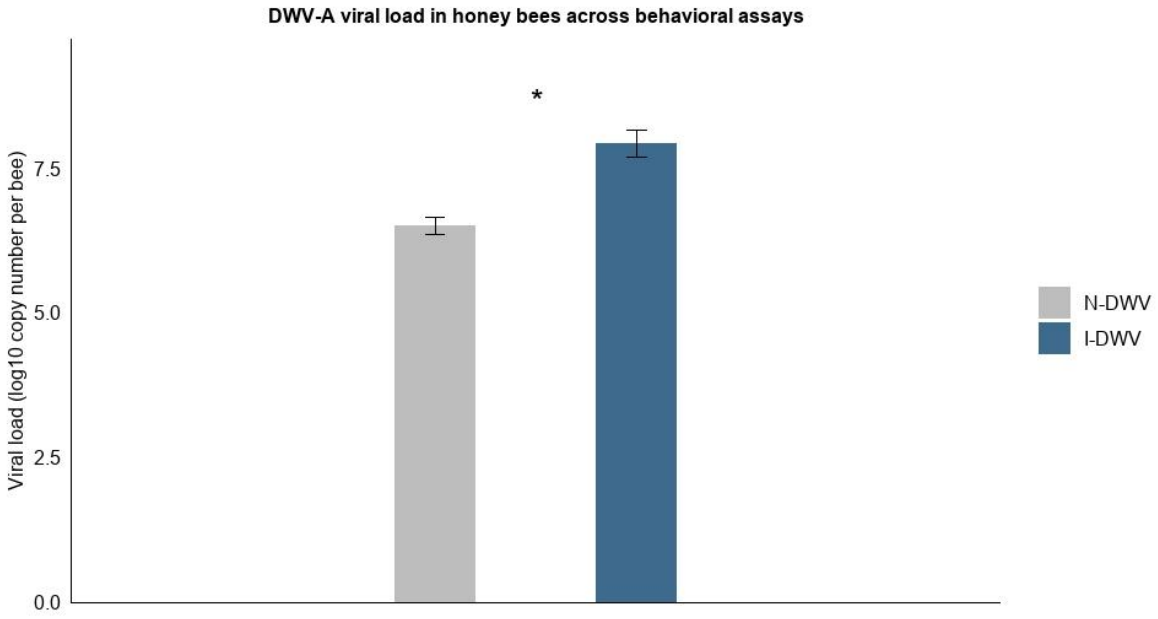

Figure S2. Quantification of DWV-A viral load in *A. mellifera* whole heads (including antennae) evaluated in the behavioral assays. Bars represent the absolute viral load (log_{10} copies/bee) at 15 days post-infection (dpi) of individuals inoculated (I-DWV) or non-inoculated (N-DWV) with Deformed wing virus variant A (DWV-A). Data show the pooled viral load of the evaluated population, grouping individuals that participated independently across the three olfactometer choice assays (facing isolated stimuli of cherry, blueberry, and cherry + 1,4-cineole). Error bars indicate the standard error of the mean (SEM). The asterisk (*) indicates statistically significant differences between the experimental groups ($p < 0.05$, Mann-Whitney *U* test).

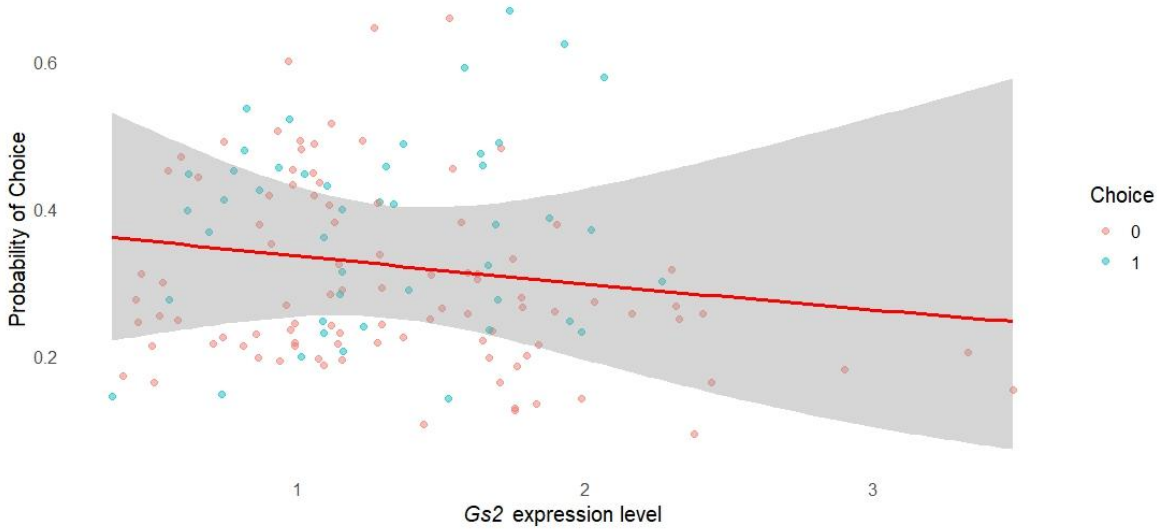

Figure S3. Probability of *A. mellifera* choosing the floral stimuli (cherry, blueberry, or a mixture of cherry + 1,4-cineole) in a Y-tube olfactometer as a function of *Gs2* gene expression. Data from the three independent olfactory assays were pooled to evaluate the overall effect of gene expression on behavioral choice. The red line represents the logistic regression model fitted between *Gs2* relative expression levels and choice. The data points correspond to individual observations (1 = choosing a floral stimulus, n = 46; 0 = no choice or choosing the control, n = 96). The shaded area indicates the 95% confidence interval.

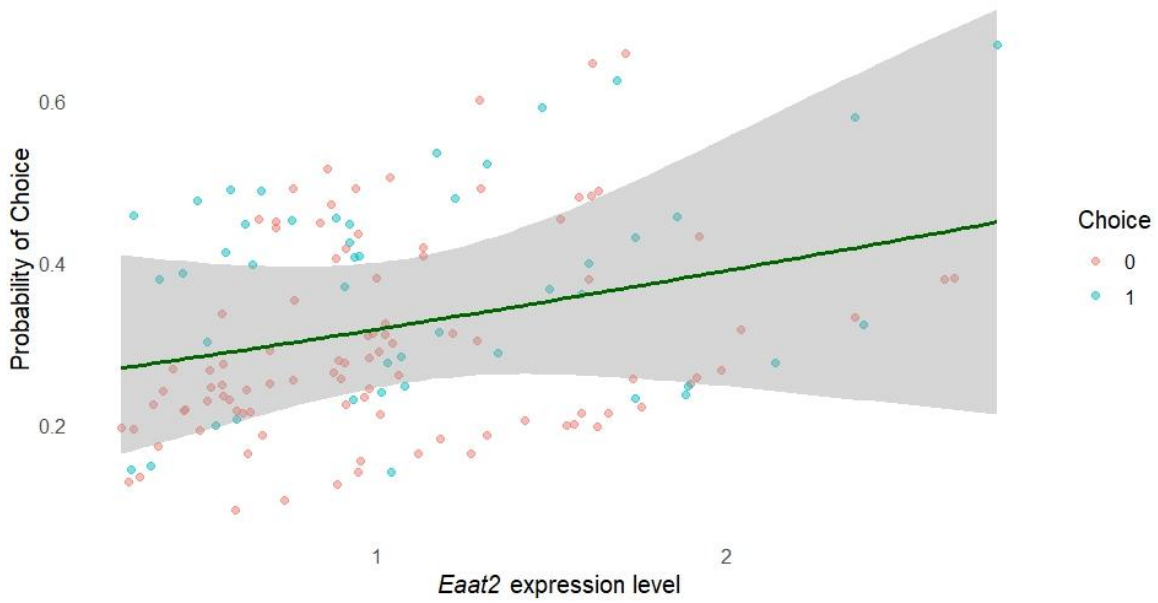

Figure S4. Probability of *A. mellifera* choosing the floral stimuli (cherry, blueberry, or a mixture of cherry + 1,4-cineole) in a Y-tube olfactometer as a function of *Eaat2* gene expression. Data from the three independent olfactory assays were pooled to evaluate the overall effect of gene expression on behavioral choice. The red line represents the logistic regression model fitted between *Eaat2* relative expression levels and choice. The data points correspond to individual observations (1 = choosing a floral stimulus, n = 46; 0 = no choice or choosing the control, n = 96). The shaded area indicates the 95% confidence interval.

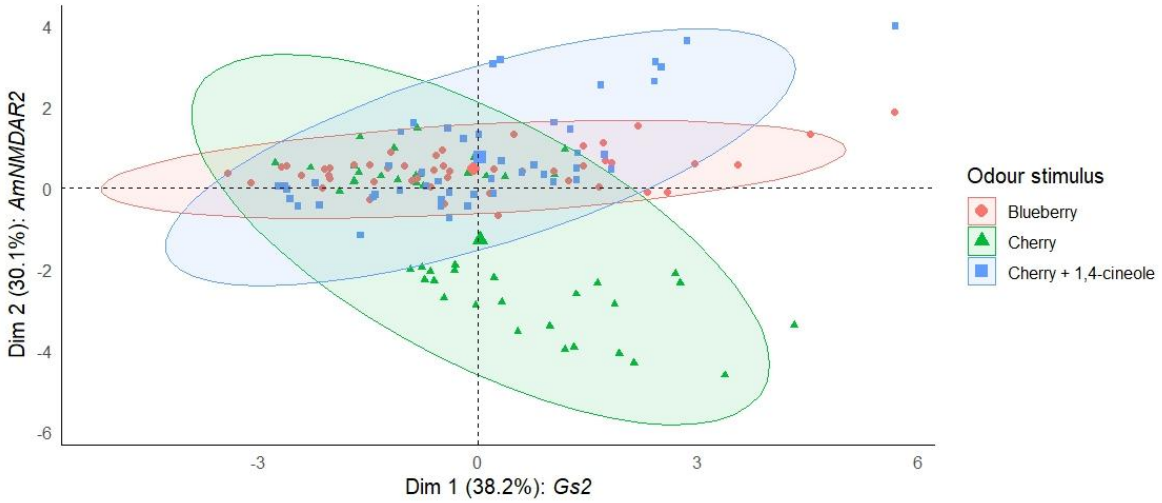

Figure S5. Principal Component Analysis (PCA) of glutamatergic gene expression profiles in *A. mellifera* in response to different olfactory stimuli: blueberry (red circles), cherry (green triangles), and cherry + 1,4-cineole (blue squares). The ellipses represent the 95% confidence intervals for each group.

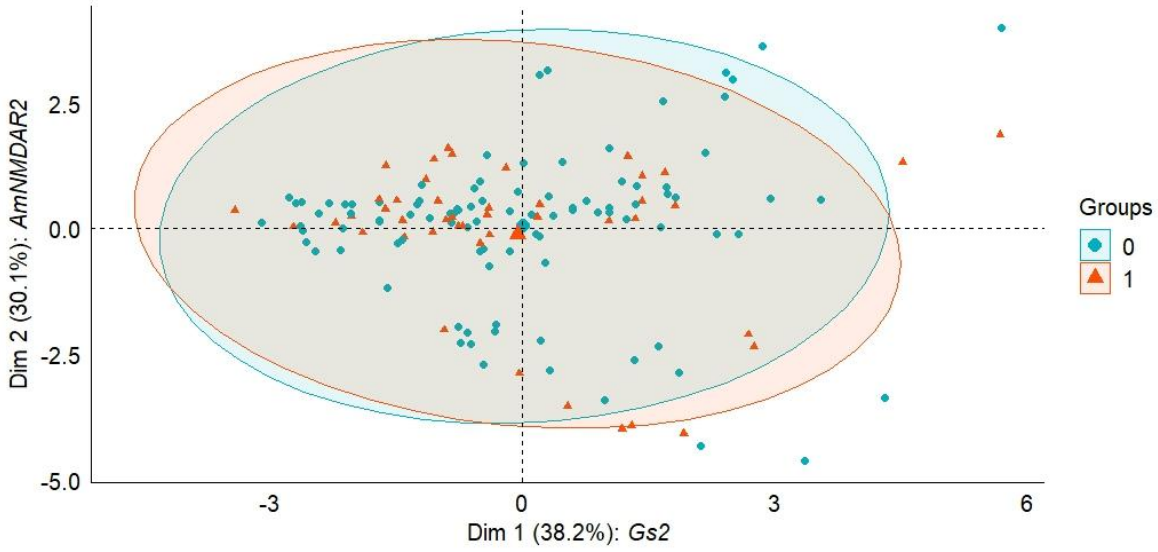

Figure S6. Principal Component Analysis (PCA) of the glutamatergic system in *A. mellifera* based on behavioral response. The points represent individuals without a preference (0, turquoise) and those with a positive preference (1, orange). The ellipses delineate the 95% confidence interval for each group.